

# Leptonic CP asymmetry and Light flavored scalar

Yoshihiko Abe<sup>\*</sup>, Toshimasa Ito<sup>†</sup>, Koichi Yoshioka<sup>‡</sup>

*Department of Physics, Kyoto University, Kyoto 606-8502, Japan*

## Abstract

We consider a situation where right-handed neutrinos couple to a light scalar which is possibly a Nambu-Goldstone boson resulting from high-energy symmetry breaking. Its coupling is typically complex-valued and flavor-dependent. In this work, we investigate the possibility of the leptonic asymmetry generation in the Universe from tree-level right-handed neutrino decay to flavorful light scalar. Furthermore a new source of asymmetry generation from a single decay process is pointed out, which is characteristic of the present setting.

arXiv:2110.11096v1 [hep-ph] 21 Oct 2021

---

<sup>\*</sup>y.abe@gauge.scphys.kyoto-u.ac.jp

<sup>†</sup>toshimasa.i@gauge.scphys.kyoto-u.ac.jp

<sup>‡</sup>yoshioka@gauge.scphys.kyoto-u.ac.jp

# Contents

<b>1</b>	<b>Introduction</b>	<b>1</b>
<b>2</b>	<b>Lagrangian and two-body decay</b>	<b>2</b>
<b>3</b>	<b>Three-body decay for asymmetry</b>	<b>5</b>
3.1	The lightest mode . . . . .	6
3.2	Heavier modes . . . . .	7
<b>4</b>	<b>Lepton asymmetry with <math>\chi</math> scalar</b>	<b>8</b>
4.1	Boltzmann equations . . . . .	8
4.2	Parameter space . . . . .	12
4.3	Property of $\chi$ scalar . . . . .	15
<b>5</b>	<b>Summary</b>	<b>17</b>
<b>A</b>	<b>Three-body decay widths</b>	<b>18</b>
<b>B</b>	<b>CP asymmetry (width differences)</b>	<b>19</b>
<b>C</b>	<b>Boltzmann equations and asymmetry formulae</b>	<b>21</b>
C.1	Boltzmann equations . . . . .	21
C.2	Phenomenological formulae for lepton asymmetry . . . . .	22
C.2.1	Case for freeze-in from $N_2$ . . . . .	23
C.2.2	Case for strong $N_1$ washout . . . . .	24

## 1 Introduction

The Standard Model (SM) of particle physics and cosmology still have some mysteries, e.g., the nature of dark matter, the source of matter-antimatter asymmetry, the origin of neutrino masses, and so on. An attractive idea to realize tiny neutrino masses is the seesaw mechanism with Majorana right-handed (RH) neutrinos [1–3], called the type I seesaw. The additional Majorana fermions can also be the origin of matter-antimatter asymmetry via their decay, the scenario called leptogenesis [4].

The baryon asymmetry in the present Universe is measured by the cosmic microwave background observation [5] as

$$Y_B = \frac{n_B}{s} = (0.852 - 0.888) \times 10^{-10}, \quad (1.1)$$

with the number density  $n_B$  and the entropy density  $s$ . In the leptogenesis scenario, the RH neutrinos generate the lepton asymmetry, which is then converted to the baryon asymmetry [6] via the sphaleron process [7]. In the simplest leptogenesis, the interference

between the tree-level and one-loop level RH neutrino two-body decays gives a source of the asymmetry, which is determined by neutrino Yukawa couplings. On the other hand, Refs. [8–13] also discuss possibilities of tree-level leptogenesis by considering various extensions of the neutrino sector.

In this paper, we focus on a possibility of flavorful light scalar for the lepton asymmetry generation. This is a minimal scalar extension of the type-I seesaw model by introducing a SM singlet scalar interacting with the RH neutrinos. This kind of scalar may be motivated by some dynamical origin of Majorana neutrino mass scale, but in this work we do not specify it and investigate the general form of scalar interaction to the RH neutrinos. In this setup, we study the tree-level leptogenesis via the RH neutrino three-body decays with this flavorful scalar field.

The rest parts are organized as follows. In Sec. 2, the model we focus on is introduced and we derive the decay widths and the asymmetry parameters of the two-body decay processes. In Sec. 3, the three-body decay widths and the asymmetry parameter are evaluated and we give their approximation formulae. In Sec. 4, we discuss the behaviors of the lepton asymmetry and its approximated relic value by solving the Boltzmann equations, and show the allowed parameter spaces of this model. We also give some comments on the dynamics of the additional singlet scalar field and its realization in some phenomenological models. Sec. 5 is devoted to the summary of this paper.

## 2 Lagrangian and two-body decay

In this work, we denote the RH neutrinos as  $N_i$  in the mass diagonal basis. They are the Majorana fermions with the Majorana masses  $m_{N_i}$ . An SM gauge singlet scalar  $\chi$  is introduced and assumed to have the coupling to the RH neutrinos. The lagrangian we consider is

$$\mathcal{L} = \mathcal{L}_{\text{SM}} + \frac{1}{2}\bar{N}_i(i\cancel{\partial} - m_{N_i})N_i - y_{ij}^\nu \tilde{H}^\dagger \bar{N}_i P_L L_j + \text{h.c.} - \frac{1}{2}\chi \bar{N}_i (\xi_{ij} P_R + \xi_{ij}^* P_L) N_j, \quad (2.1)$$

where  $L_j$  mean the SM lepton doublets and  $H$  the Higgs one, and  $P_{L/R}$  is the chirality projection operator. The coupling constants  $\xi_{ij}$  are  $i, j$  symmetric and generally complex-valued. They can be decomposed into the scalar (real part) and pseudo-scalar (imaginary part) couplings to  $N_i$ . As discussed in Ref. [14], with the seesaw relation, the neutrino Yukawa coupling  $y^\nu$  can be generally parameterized as

$$y^\nu = \frac{\sqrt{2}i}{v} \sqrt{M_N} R \sqrt{m_\nu} U_{\text{MNS}}^\dagger, \quad (2.2)$$

with the Majorana mass matrix  $M_N = \text{diag}(m_{N_1}, m_{N_2}, m_{N_3})$  and the neutrino mass matrix  $m_\nu = \text{diag}(m_{\nu_1}, m_{\nu_2}, m_{\nu_3})$ , and the neutrino flavor mixing matrix  $U_{\text{MNS}}$ .  $v \approx 246$  GeV is the electroweak scale. For the neutrino masses and mixing angles, we use the experimentally observed values summarized in Ref. [15].  $R$  is an arbitrary complex orthogonal

matrix describing the degrees of freedom of neutrino Yukawa couplings which cannot be reached with the seesaw relation. We parameterize  $R$  as

$$R = \begin{pmatrix} 1 & 0 & 0 \\ 0 & \cos \omega_{23} & \sin \omega_{23} \\ 0 & -\sin \omega_{23} & \cos \omega_{23} \end{pmatrix} \begin{pmatrix} \cos \omega_{13} & 0 & \sin \omega_{13} \\ 0 & 1 & 0 \\ -\sin \omega_{13} & 0 & \cos \omega_{13} \end{pmatrix} \begin{pmatrix} \cos \omega_{12} & \sin \omega_{12} & 0 \\ -\sin \omega_{12} & \cos \omega_{12} & 0 \\ 0 & 0 & 1 \end{pmatrix}, \quad (2.3)$$

introducing the complex angles  $\omega_{ij}$  (called the Casas-Ibarra (CI) parameters in the following).

Through the neutrino Yukawa coupling, the RH neutrinos interact with the SM thermal bath. For the two-body decay of  $N_i$  to the SM particles, the partial widths at tree level are given by

$$\Gamma_{N_i \rightarrow L_j H} = \Gamma_{N_i \rightarrow \bar{L}_j \bar{H}} = \frac{y_{ij}^\nu y_{ji}^{\nu\dagger}}{16\pi} m_{N_i}, \quad (2.4)$$

where  $\bar{L}$ ,  $\bar{H}$  means the corresponding anti-particles. We denote the total width of the two-body decay via neutrino Yukawa coupling as

$$\tilde{\Gamma}_i = \sum_j (\Gamma_{N_i \rightarrow L_j H} + \Gamma_{N_i \rightarrow \bar{L}_j \bar{H}}). \quad (2.5)$$

When  $m_{N_2} > m_{N_1} + m_\chi$ , a heavier mode  $N_2$  can also decay to  $N_1$  and  $\chi$  via the off-diagonal coupling  $\xi_{12}$  and its width is evaluated as

$$\Gamma_{N_2 \rightarrow N_1 \chi} = \frac{m_{N_2}}{16\pi} \frac{\sqrt{\lambda(m_{N_2}^2, m_{N_1}^2, m_\chi^2)}}{m_{N_2}^2} \left\{ \left[ \left(1 - \frac{m_{N_1}}{m_{N_2}}\right)^2 - \frac{m_\chi^2}{m_{N_2}^2} \right] (\text{Im } \xi_{12})^2 + \left[ \left(1 + \frac{m_{N_1}}{m_{N_2}}\right)^2 - \frac{m_\chi^2}{m_{N_2}^2} \right] (\text{Re } \xi_{12})^2 \right\}, \quad (2.6)$$

with the kinematic function  $\lambda(x, y, z) = x^2 + y^2 + z^2 - 2xy - 2yz - 2yx$ .

As we will see in the following, the decay of the lightest  $N_1$  is dominated by the two-body decay, but for a heavier mode the resonant contribution of three-body decay is comparable to that of  $N_2 \rightarrow N_1 \chi$ . Then the total decay widths  $\Gamma_{N_i}$  of the lightest and heavier RH neutrinos are generally written by

$$\Gamma_{N_1} \approx \tilde{\Gamma}_1, \quad \Gamma_{N_2} = \tilde{\Gamma}_2 + \Gamma_{N_2 \rightarrow N_1 \chi} + \Gamma_2, \quad (2.7)$$

where  $\Gamma_i$  are the three-body decay widths of  $N_i$  and will be described in the next section.

The CP asymmetry in the ordinary leptogenesis comes from the interference of the RH neutrino's two-body decays (the tree-level and the right two diagrams in Fig. 1), where the phases of neutrino Yukawa couplings play an important role. The asymmetry parameters  $\tilde{\epsilon}_i^{(LH)}$  associated with this interference is evaluated as (for a review [16]),

$$\tilde{\epsilon}_i^{(LH)} = \frac{\Gamma_{N_i \rightarrow LH} - \Gamma_{N_i \rightarrow \bar{L}\bar{H}}}{\Gamma_{N_i \rightarrow LH} + \Gamma_{N_i \rightarrow \bar{L}\bar{H}}} = \frac{1}{8\pi (y^\nu y^{\nu\dagger})_{ii}} \sum_j \text{Im} [(y^\nu y^{\nu\dagger})_{ji}]^2 g(m_{N_j}^2/m_{N_i}^2), \quad (2.8)$$

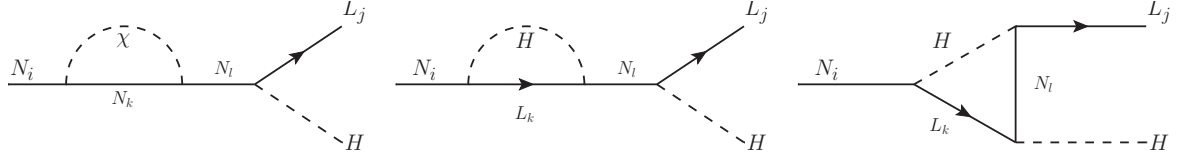


Figure 1: The one-loop two-body decays of a RH neutrino  $N_i$  to the SM fields. (Left) from lighter RH neutrinos and the scalar  $\chi$ . (Middle and Right) from the SM loops.

where  $g(x)$  in the SM is given by  $g(x) = \sqrt{x} \left[ \frac{2-x}{1-x} - (1+x) \ln \left( \frac{1+x}{x} \right) \right]$ . It is noticed that, when  $\omega_{ij}$  are real or pure imaginary,  $\tilde{c}_i^{(LH)}$  vanish and the two-body decay via the neutrino Yukawa loop does not generate the CP asymmetry.

In addition to the SM particle loops, lighter RH neutrinos and the scalar field  $\chi$  give an additional asymmetry in the two-body decay of heavier RH neutrinos. The left diagram in Fig. 1 shows the relevant one-loop contribution to the  $N_i$  decay. The asymmetry reads from the difference between the decay widths to particles and anti-particles,

$$\Delta\Gamma_{N\chi} = |\mathcal{M}_0 + \mathcal{M}_1|^2 - |\mathcal{M}_0^C + \mathcal{M}_1^C|^2, \quad (2.9)$$

where  $\mathcal{M}_0^{(C)}$  denotes the amplitude of the tree-level decay to the (anti-)particles and  $\mathcal{M}_1^{(C)}$  that of the one-loop diagram including  $\chi$ , respectively. This is evaluated as

$$\Delta\Gamma_{N\chi} = \frac{m_{N_i}^4}{4\pi^2} \sum_{k,l} \frac{1}{m_{N_i}^2 - m_{N_k}^2} \int_0^1 dx \operatorname{Im}(\ln \Delta_{N_k\chi}^2) \operatorname{Im}[f_{li}(x)(y^\nu y^{\nu\dagger})_{il}], \quad (2.10)$$

where

$$\Delta_{N_k\chi}^2 = x(x-1)m_{N_i}^2 + (1-x)m_{N_k}^2 + xm_\chi^2, \quad (2.11)$$

$$f_{li}(x) = \left( \xi_{lk}^* \xi_{ki} + \xi_{lk} \xi_{ki}^* \frac{m_{N_l}}{m_{N_i}} \right) x + \xi_{lk}^* \xi_{ki}^* \frac{m_{N_k}}{m_{N_i}} + \xi_{lk} \xi_{ki} \frac{m_{N_k} m_{N_l}}{m_{N_i}^2}. \quad (2.12)$$

In order to produce non-trivial asymmetry, the conditions  $i \neq k$  for the interference and  $\Delta_{N_k\chi}^2 < 0$  are needed. The latter condition is satisfied if the internal loop particles  $N_k$  and  $\chi$  are lighter than the parent particle  $N_i$ , and then only the case of  $i = 2$ ,  $k = l = 1$  gives a non-vanishing asymmetry parameter. As a result, we obtain the  $N$ - $\chi$  loop contribution to asymmetry parameter

$$\tilde{\epsilon}_2^{(N\chi)} = \frac{-m_{N_2}}{64\pi^2 \tilde{\Gamma}_2} \int_{x_-}^{x_+} dx \operatorname{Im}[f_{12}(x)(y^\nu y^{\nu\dagger})_{21}] \approx \frac{1}{16\pi(y^\nu y^{\nu\dagger})_{22}} \operatorname{Im}[\xi_{11} \xi_{12}^* (y^\nu y^{\nu\dagger})_{12}], \quad (2.13)$$

where  $x_\pm$  are the solutions for  $\Delta_{N_1\chi}^2 = 0$ . In the latter approximation, we have assumed the hierarchy  $m_{N_1} \ll m_{N_2}$ . The total CP asymmetry from two-body decay of the lightest and heavier RH neutrinos are given by

$$\tilde{\epsilon}_1 = \tilde{\epsilon}_1^{(LH)}, \quad \tilde{\epsilon}_2 = \tilde{\epsilon}_2^{(LH)} + \tilde{\epsilon}_2^{(N\chi)}. \quad (2.14)$$

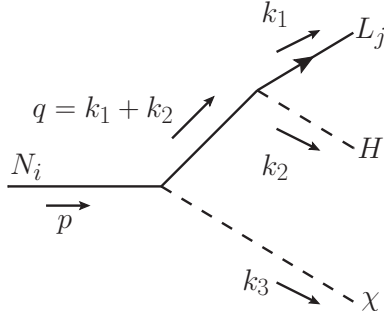


Figure 2: The three-body decay of a RH neutrino  $N_i$  at tree level including the scalar  $\chi$ .

With general complex phases of neutrino Yukawa couplings,  $\tilde{\epsilon}_i^{(LH)}$  are not necessarily vanishing simultaneously. In the following analysis, we simply assume that the CI parameters are real or pure imaginary to examine the CP asymmetry effect of the flavorful scalar  $\chi$ .

### 3 Three-body decay for asymmetry

When there exist a scalar  $\chi$  and its (pseudo-) scalar coupling to the RH neutrinos  $N$ , non-trivial CP asymmetry can be generated at the three-body decay  $N \rightarrow LH\chi$  (Fig. 2). Its amplitude is

$$\mathcal{M}_{N_i \rightarrow L_j H \chi} = - \sum_k \overline{u_{L_j}}(k_1) y_{jk}^{\nu \dagger} P_R \frac{1}{\not{q} - \bar{m}_{N_k}} (\xi_{ki} P_R + \xi_{ki}^* P_L) u_{N_i}(p), \quad (3.1)$$

where  $\bar{m}_{N_k} = m_{N_k} - i\Gamma_{N_k}/2$ . The initial and final state momenta  $p$ ,  $k_i$  are shown in the figure ( $q = k_1 + k_2$ ). The renormalized mass parameters are  $m_{N_i}^r = m_{N_i}^2 - \Gamma_{N_i}^2/4$  for  $\Gamma_{N_i}$  being the width of the resonance  $N_i$ , but we quantitatively drop any difference of  $\mathcal{O}((\Gamma/m_N)^2)$  throughout this paper. Summing up the final charged-lepton flavor and gauge charge, the three-body decay width becomes

$$\begin{aligned} \Gamma_{N_i \rightarrow LH\chi} = & \sum_{k,l} \frac{(y^\nu y^{\nu \dagger})_{lk}}{256\pi^3 m_{N_i}^3} \int_0^{(m_{N_i} - m_\chi)^2} dm_{12}^2 \int_{[m_{23}]_-}^{[m_{23}]_+} dm_{23}^2 \frac{1}{(m_{12}^2 - \bar{m}_{N_l}^{*2})(m_{12}^2 - \bar{m}_{N_k}^2)} \\ & \times \left[ \xi_{il} \xi_{ki}^* m_{12}^2 (m_{12}^2 + m_{23}^2 - m_\chi^2) + (\xi_{il} \xi_{ki} \bar{m}_{N_k} + \xi_{il}^* \xi_{ki}^* \bar{m}_{N_l}^*) m_{N_i} m_{12}^2 \right. \\ & \left. + \xi_{il}^* \xi_{ki} \bar{m}_{N_l}^* \bar{m}_{N_k} (m_{N_i}^2 - m_{23}^2) \right]. \end{aligned} \quad (3.2)$$

The invariant mass parameters are defined by  $m_{12}^2 = (k_1 + k_2)^2$ ,  $m_{23}^2 = (k_2 + k_3)^2$ , and the maximum and minimum values of  $m_{23}^2$  with a fixed  $s$  are given by [15, 17]

$$[m_{23}^2]_{\pm} = \frac{1}{2} \left[ m_{N_i}^2 + m_\chi^2 - m_{12}^2 \pm \sqrt{\lambda(m_{N_i}^2, m_\chi^2, m_{12}^2)} \right]. \quad (3.3)$$

The three-body decay to the anti-particles  $\Gamma_{N_i \rightarrow \bar{L}\bar{H}\chi}$  is evaluated in the same manner. The total decay width and the CP asymmetry parameter for the three-body decay are defined by

$$\Gamma_i = \Gamma_{N_i \rightarrow LH\chi} + \Gamma_{N_i \rightarrow \bar{L}\bar{H}\chi}, \quad \epsilon_i = \frac{\Gamma_{N_i \rightarrow LH\chi} - \Gamma_{N_i \rightarrow \bar{L}\bar{H}\chi}}{\Gamma_{N_i \rightarrow LH\chi} + \Gamma_{N_i \rightarrow \bar{L}\bar{H}\chi}}. \quad (3.4)$$

In the following, we will discuss dominant contributions to the widths and asymmetry parameters and their approximate forms.

### 3.1 The lightest mode

Among the intermediate states  $N_k$ , the lightest one  $N_1$  generally gives the dominant contribution to the  $N_1$  three-body decay, i.e., the  $i = k = l = 1$  part in (3.2). For a typical hierarchy of mass parameters,  $m_\chi \ll m_{N_1} \ll m_{N_2}$ , the  $N_1$  decay width reduces to

$$\Gamma_1^{(11)} \approx \frac{m_{N_1}}{64\pi^3} (y^\nu y^{\nu\dagger})_{11} [|\xi_{11}|^2 + \text{Re}(\xi_{11}^2)] \ln\left(\frac{m_{N_1}}{m_\chi}\right), \quad (3.5)$$

which is mainly determined by the diagonal coupling  $\xi_{11}$ . Compared with the two-body decay  $N_1 \rightarrow LH$ , the width is multiplied by a factor  $\sim (\xi_{11})^2/4\pi \ln(m_{N_1}/m_\chi)$ , which can be of order one. If  $\xi_{11}$  is negligibly small, the width is instead given by the  $k = l = 2$  part,

$$\Gamma_1^{(22)} \approx \frac{m_{N_1}^3}{384\pi^3 m_{N_2}^2} (y^\nu y^{\nu\dagger})_{22} |\xi_{12}|^2. \quad (3.6)$$

The CP asymmetry, the difference between the decay widths to particles and anti-particles, is usually described by the quantum interference of processes with different intermediate states. For the current three-body decay, such interference occurs from the diagrams with different intermediate neutrinos  $N_{k,l}$  ( $k \neq l$ ), that is, the cross terms in the amplitude squared. It is important that, in addition to this usual asymmetry, the present model induces CP asymmetry from a single diagram with one intermediate state. For example, we find the  $N_1$  three-body decay with virtual  $N_1$  generates a nonzero CP asymmetry parameter

$$\epsilon_1^{(11)} \approx \frac{\text{Im}(\xi_{11}^2)}{|\xi_{11}|^2 + \text{Re}(\xi_{11}^2)} \frac{\Gamma_{N_1}}{2m_{N_1}}, \quad (3.7)$$

which is irrelevant to the  $N_2$  physics at the leading order. (This is the approximate formula for  $m_\chi \ll m_{N_1} \ll m_{N_2}$ . The exact form of asymmetry parameter is found in Appendix B.)

The non-vanishing ‘‘interference’’ from a single diagram (3.7) is a characteristic feature of the present decay mode and its origin is understood by the amplitude form. The three-body decay amplitude (3.1) contains the factor  $P_R(\not{q} + \bar{m}_N)(\xi P_R + \xi^* P_L)$  between the initial and final spinor wavefunctions. The first projection  $P_R$  comes from the Yukawa

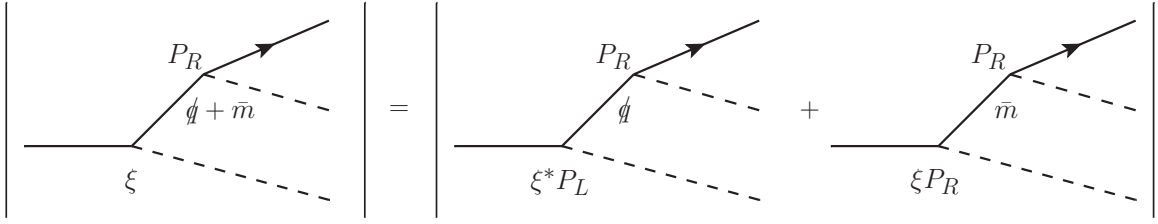


Figure 3: CP asymmetry (cross term) from a single amplitude squared.

(chirality-violating) vertex, the second factor ( $q + \bar{m}_N$ ) the propagator of heavy unstable fermion, and the third one ( $\xi P_R + \xi^* P_L$ ) means the Majorana fermion vertex. The chirality structure implies this factor is divided into two pieces  $\bar{m}_N \xi$  and  $q \xi^*$ , and hence the squared amplitude generally contains a cross term of these two pieces (Fig. 3). Further the corresponding decay width to anti-particles is obtained by the replacement of couplings  $\xi \leftrightarrow \xi^*$  (and  $y^\nu \leftrightarrow y^{\nu*}$ ,  $P_R \leftrightarrow P_L$ ). In the end, the interference of these two pieces leads to the CP asymmetry proportional to  $\text{Im}(\xi^2) \text{Im}(\bar{m})$ , appearing in the numerator of (3.7). We thus find that this CP asymmetry from a single decay process is generated in the presence of a chiral vertex, a unstable intermediate state, and a complex decay coupling. The three-body decay of a RH neutrino to the SM particles plus scalar is an interesting realization of all these criteria satisfied.

The interference of different intermediate states also contributes to the CP asymmetry as usual, and its approximate form is found

$$\epsilon_1^{(12)} \approx \frac{m_{N_1} \Gamma_{N_2}}{8m_{N_2}^2} \frac{\text{Im}[(y^\nu y^{\nu\dagger})_{12} \xi_{12} (2\xi_{11} + 3\xi_{11}^*)]}{(y^\nu y^{\nu\dagger})_{11} [|\xi_{11}|^2 + \text{Re}(\xi_{11}^2)] \ln\left(\frac{m_{N_1}}{m_\chi}\right)}. \quad (3.8)$$

Which contribution (3.7) or (3.8) is the dominant CP asymmetry depends on the model parameters.

The  $k = l = 2$  part in the  $N_1$  decay width only gives a subdominant CP asymmetry in almost case due to the large  $m_{N_2}$  suppression.

### 3.2 Heavier modes

A heavier RH neutrino than  $N_1$  can also generate CP asymmetry at its three-body decay. A lighter intermediate state, e.g.,  $N_1$  meets the resonance around its mass  $m_{12}^2 \sim m_{N_1}^2$  and then the amplitude is largely enhanced. There are two types of enhancement in the decay width (3.2), the  $k = l = 1$  and cross terms. The enhanced contributions to the decay width are evaluated with the narrow width approximation. For the  $k = l = 1$  part, we obtain

$$\Gamma_2^{(11)} = \frac{m_{N_1}}{128\pi^3 m_{N_2}^3 \Gamma_{N_1}} (y^\nu y^{\nu\dagger})_{11} \sqrt{\lambda(m_{N_1}^2, m_{N_2}^2, m_\chi^2)} \\ \times [|\xi_{12}|^2 (m_{N_1}^2 + m_{N_2}^2 - m_\chi^2) + 2 \text{Re}(\xi_{12}^2) m_{N_1} m_{N_2}], \quad (3.9)$$



where we have neglected  $\mathcal{O}((\Gamma_{N_1})^2)$  terms. In the limit  $m_\chi \ll m_{N_1} \ll m_{N_2}$  and  $\Gamma_{N_1} \approx \tilde{\Gamma}_1$ , the  $N_1$  resonant contribution (3.9) is equal to  $\frac{1}{2}\Gamma_{N_2 \rightarrow N_1 \chi}$ . (The prefactor  $\frac{1}{2}$  implies  $\tilde{\Gamma}_1$  contains the decays both to particles and anti-particles.) We also find the cross-term contribution is relatively suppressed than the  $k = l = 1$  one. The enhanced on-shell decay (3.9) is controlled by the off-diagonal coupling  $\xi_{12}$ . When  $\xi_{12}$  is negligibly small, the  $N_2$  three-body decay width is dominantly given by the non-resonant  $k = l = 2$  part and its approximate form is

$$\Gamma_2^{(22)} \approx \frac{m_{N_2}}{64\pi^3} (y^\nu y^{\nu\dagger})_{22} [|\xi_{22}|^2 + \text{Re}(\xi_{22}^2)] \ln\left(\frac{m_{N_2}}{m_\chi}\right). \quad (3.10)$$

The CP asymmetry of  $N_2$  three-body decay is also generated by the resonant and non-resonant parts. The asymmetry from the  $N_1$  resonant part comes from the last term in (3.9) and reads

$$\epsilon_2^{(11)} = \frac{m_{N_1}}{128\pi^2 m_{N_2}^2 \Gamma_2} (y^\nu y^{\nu\dagger})_{11} \sqrt{\lambda(m_{N_1}^2, m_{N_2}^2, m_\chi^2)} \text{Im}(\xi_{12})^2. \quad (3.11)$$

The usual interference of different diagrams also contributes to the asymmetry and is approximately found

$$\epsilon_2^{(12)} \approx \frac{-m_{N_1}}{128\pi^2 \Gamma_2} \text{Im} [(y^\nu y^{\nu\dagger})_{21} \xi_{22}^* \xi_{12}] \quad (3.12)$$

in the limit  $m_{N_1} \ll m_{N_2}$ . This usual cross-term part gives a tiny contribution to the decay width as mentioned above, but a possibly large one to the CP asymmetry parameter. The exact form of asymmetry parameters from the resonant contribution is found in Appendix B.

Similar to the  $N_1$  decay, there is the CP asymmetry from a single diagram where the unstable  $N_2$  is the intermediate state. In this case, the difference of the decay widths to particles and anti-particles is the same form as in the  $N_1$  decay, but the total three-body decay width has several possibilities as described above. The resultant asymmetry parameter from the  $N_2$ -intermediate diagram becomes

$$\epsilon_2^{(22)} \approx \frac{\Gamma_{N_2}}{128\pi^3 \Gamma_2} (y^\nu y^{\nu\dagger})_{22} \text{Im}(\xi_{22}^2) \ln\left(\frac{m_{N_2}}{m_\chi}\right) \quad (3.13)$$

Among the above 3 types of  $\epsilon_2$ , the leading contribution is generally given by the non-resonant part (3.13) except for a tiny  $\xi_{22}$  (see Fig. 4). We thus find for the  $N_2$  three-body decay that the width is determined by the diagonal  $k = l = 1$  or  $k = l = 2$  part, and the CP asymmetry is governed by the non-resonant  $k = l = 2$  part.

## 4 Lepton asymmetry with $\chi$ scalar

### 4.1 Boltzmann equations

In this section, solving the Boltzmann equations in the present system, we discuss the time evolution of yields and the washout effect of asymmetry. When the temperature of

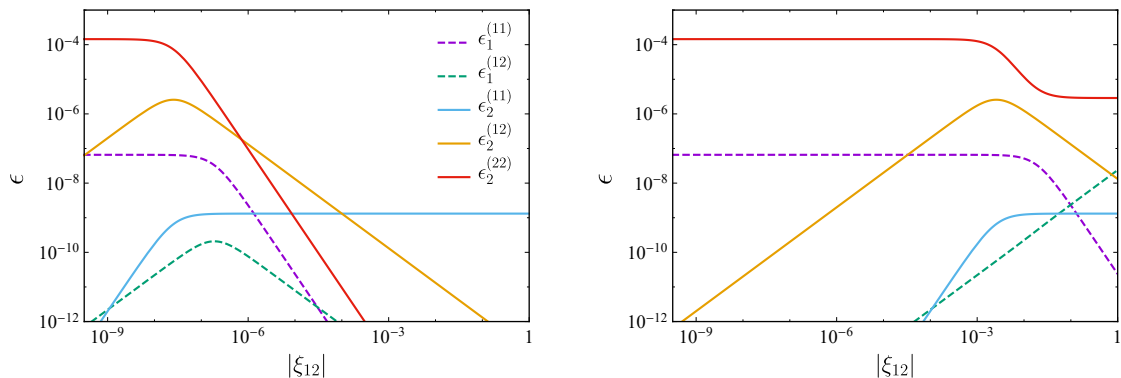


Figure 4: A typical comparison of various asymmetry parameters. The approximate formulae of these parameters are given in the text. (Left)  $|\xi_{11}| = |\xi_{22}| = 10^{-5}$ . (Right)  $|\xi_{11}| = |\xi_{22}| = 1$ . In these figures, the neutrino Yukawa couplings are roughly replaced by the mass eigenvalues of neutrinos as  $(y^\nu y^{\nu\dagger})_{ij} \sim (m_{N_i} m_{N_j} m_{\nu_i} m_{\nu_j})^{1/2}/v^2$ , and the complex phases of couplings are assumed such that the asymmetry parameters take their maximal values.

the Universe is denoted by  $T$ , the Hubble parameter  $H$  and the entropy density  $s$  in the radiation-dominated Universe are defined by

$$H(T) = \sqrt{\frac{\pi^2}{90} g_*} \frac{T^2}{M_P}, \quad s(T) = \frac{2\pi^2}{45} g_*^S T^3, \quad (4.1)$$

where  $M_P = 2.44 \times 10^{18}$  GeV is the reduced Planck scale,  $g_*$  ( $g_*^S$ ) denotes the effective degrees of freedom for the energy (entropy) density. The yield of particle  $i$  is defined by  $Y_i = n_i/s$  with the number density  $n_i$ , and  $Y_i^{\text{eq}}$  is that of the thermal equilibrium.

In the following analysis, we apply for simplicity the single flavor approximation to the lepton asymmetry, and write the yields of leptons and anti-leptons as

$$Y_L = Y_L^{\text{eq}} + \frac{1}{2} Y_{\Delta L}, \quad Y_{\bar{L}} = Y_L^{\text{eq}} - \frac{1}{2} Y_{\Delta L}, \quad (4.2)$$

where  $Y_{\Delta L}$  denotes the yield of the lepton asymmetry. If one would like to include flavor-dependent effects, a further detailed analysis with, e.g., the density matrix formalism, is needed [18], but that is beyond the purpose of this work. The SM particles including the leptons and the Higgs field are assumed to be in the thermal bath. In this setup, the Boltzmann equations needed for the lepton asymmetry are given by

$$\begin{aligned} Hx \frac{dY_{N_1}}{dx} &\approx \frac{K_1(m_{N_1}/T)}{K_2(m_{N_1}/T)} Y_{N_1}^{\text{eq}} \left[ \tilde{\Gamma}_1 \left( 1 - \frac{Y_{N_1}}{Y_{N_1}^{\text{eq}}} \right) - \frac{1}{2} \tilde{\Gamma}_1 \tilde{\epsilon}_1 \frac{Y_{\Delta L}}{Y_L^{\text{eq}}} + \Gamma_1 \left( -\frac{Y_{N_1}}{Y_{N_1}^{\text{eq}}} + \frac{Y_\chi}{Y_\chi^{\text{eq}}} \right) \right. \\ &\quad \left. - \frac{1}{2} \Gamma_1 \epsilon_1 \frac{Y_\chi}{Y_\chi^{\text{eq}}} \frac{Y_{\Delta L}}{Y_L^{\text{eq}}} \right] + \frac{K_1(m_{N_2}/T)}{K_2(m_{N_2}/T)} Y_{N_2}^{\text{eq}} \Gamma_{N_2 \rightarrow N_1 \chi} \left( \frac{Y_{N_2}}{Y_{N_2}^{\text{eq}}} - \frac{Y_{N_1}}{Y_{N_1}^{\text{eq}}} \frac{Y_\chi}{Y_\chi^{\text{eq}}} \right), \quad (4.3) \\ Hx \frac{dY_{N_2}}{dx} &\approx \frac{K_1(m_{N_2}/T)}{K_2(m_{N_2}/T)} Y_{N_2}^{\text{eq}} \left[ \tilde{\Gamma}_2 \left( 1 - \frac{Y_{N_2}}{Y_{N_2}^{\text{eq}}} \right) - \frac{1}{2} \tilde{\Gamma}_2 \tilde{\epsilon}_2 \frac{Y_{\Delta L}}{Y_L^{\text{eq}}} + \Gamma_2 \left( -\frac{Y_{N_2}}{Y_{N_2}^{\text{eq}}} + \frac{Y_\chi}{Y_\chi^{\text{eq}}} \right) \right. \end{aligned}$$

	$N_2$ decay dominant	$N_1$ decay dominant
weak washout	$\mathcal{Y}_{\Delta L}^{\text{FI}}(z_1)$	$Y_{\Delta L}^{\text{FI}}(\infty)$
strong washout	—	$\mathcal{Y}_{\Delta L}^{\text{WO}}(\infty)$

Table 1: Four possible patterns of dominant contributions to the lepton asymmetry.

$$- \frac{1}{2} \Gamma_2 \epsilon_2 \frac{Y_\chi}{Y_\chi^{\text{eq}}} \frac{Y_{\Delta L}}{Y_L^{\text{eq}}} - \Gamma_{N_2 \rightarrow N_1 \chi} \left( \frac{Y_{N_2}}{Y_{N_2}^{\text{eq}}} - \frac{Y_{N_1}}{Y_{N_1}^{\text{eq}}} \frac{Y_\chi}{Y_\chi^{\text{eq}}} \right), \quad (4.4)$$

$$Hx \frac{dY_{\Delta L}}{dx} \approx \sum_i \frac{K_1(m_{N_i}/T)}{K_2(m_{N_i}/T)} Y_{N_i}^{\text{eq}} \left[ \tilde{\Gamma}_i \tilde{\epsilon}_i \left( \frac{Y_{N_i}}{Y_{N_i}^{\text{eq}}} - 1 \right) - \frac{1}{2} \tilde{\Gamma}_i \frac{Y_{\Delta L}}{Y_L^{\text{eq}}} \right. \\ \left. + \Gamma_i \epsilon_i \left( \frac{Y_{N_i}}{Y_{N_i}^{\text{eq}}} - \frac{Y_\chi}{Y_\chi^{\text{eq}}} \right) - \frac{1}{2} \Gamma_i \frac{Y_\chi}{Y_\chi^{\text{eq}}} \frac{Y_{\Delta L}}{Y_L^{\text{eq}}} \right], \quad (4.5)$$

$$Hx \frac{dY_\chi}{dx} \approx \sum_i \frac{K_1(m_{N_i}/T)}{K_2(m_{N_i}/T)} Y_{N_i}^{\text{eq}} \left[ \Gamma_i \left( \frac{Y_{N_i}}{Y_{N_i}^{\text{eq}}} - \frac{Y_\chi}{Y_\chi^{\text{eq}}} \right) + \frac{1}{2} \Gamma_i \epsilon_i \frac{Y_\chi}{Y_\chi^{\text{eq}}} \frac{Y_{\Delta L}}{Y_L^{\text{eq}}} \right] \\ + Y_{N_2}^{\text{eq}} \frac{K_1(m_{N_2}/T)}{K_2(m_{N_2}/T)} \Gamma_{N_2 \rightarrow N_1 \chi} \left( \frac{Y_{N_2}}{Y_{N_2}^{\text{eq}}} - \frac{Y_{N_1}}{Y_{N_1}^{\text{eq}}} \frac{Y_\chi}{Y_\chi^{\text{eq}}} \right), \quad (4.6)$$

where the dimensionless parameter  $x$  is introduced by  $x = m_{N_1}/T$ ,  $K_n(z)$  denotes the modified Bessel function of second kind, and off-shell scattering contributions are dropped for simplifying the analysis. For the three-body decay process, the on-shell contributions of RH neutrinos are deducted in order to avoid the double counting when deriving the Boltzmann equations (4.3)–(4.6).

The RH neutrinos are first generated by their interactions to the thermal bath, and the lepton asymmetry and the scalar  $\chi$  are produced via the RH neutrino decays. While the total amounts of the lepton asymmetry and  $\chi$  are related, the washout (inverse decay) effect via the neutrino Yukawa couplings deduces only the asymmetry. The Boltzmann equation for the lepton asymmetry approximately becomes

$$\frac{dY_{\Delta L}}{dx} \approx \sum_i \frac{1}{Hx} \frac{K_1(m_{N_i}x/m_{N_1})}{K_2(m_{N_i}x/m_{N_1})} \left[ \Gamma_i \epsilon_i \left( Y_{N_i} - \frac{Y_{N_i}^{\text{eq}} Y_\chi}{Y_\chi^{\text{eq}}} \right) - \frac{1}{2} \left( \tilde{\Gamma}_i + \Gamma_i \frac{Y_\chi}{Y_\chi^{\text{eq}}} \right) \frac{Y_{N_i}^{\text{eq}}}{Y_L^{\text{eq}}} Y_{\Delta L} \right],$$

where the  $\tilde{\epsilon}_i$  terms have been dropped since we are interested in the asymmetry produced by the three-body decay process. The first term of RHS produces the asymmetry via the  $N_i$  decay and the second term denotes the washout term. Depending on the  $N_1$  or  $N_2$  decay process being dominant to the production and the washout effect being strong or weak, there are four possibilities of the main lepton asymmetry as listed in Table 1. We also show in Fig. 5 the typical time evolution of the yields corresponding to these four patterns, respectively. The top panels in Fig. 5 are the results for the weak washout, and the bottom panels are for the strong one. Further, the  $N_2$  decay process is the main contribution to the asymmetry in the left panels in Fig. 5 and the  $N_1$  process is dominant

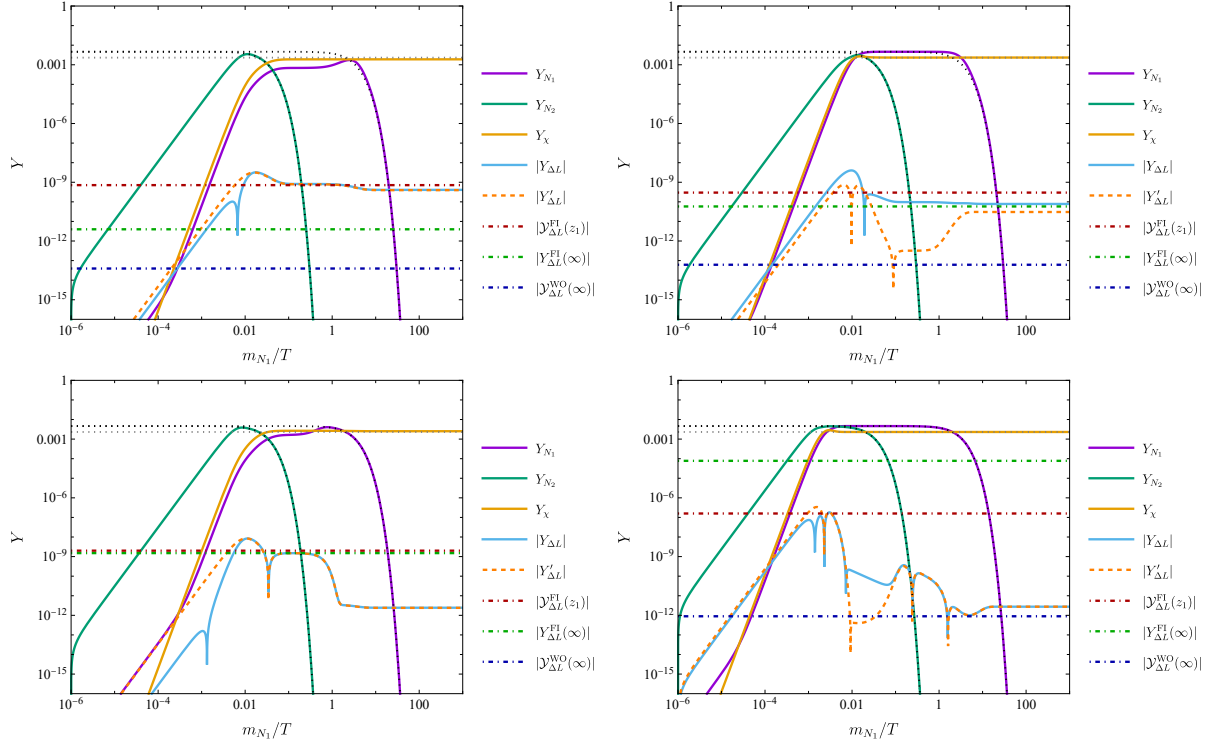


Figure 5: The time evolution of the yields. In the top panels, the washout effect is weak and the asymmetry is produced by the freeze-in mechanism of the RH neutrino decays. The washout works well in the bottom panels. In the left panels, the  $N_2$  decay is the dominant production channels and  $N_1$  dominant in the right panels. The solid lines are numerical solutions of the Boltzmann equations [Eqs. (4.3)–(4.6)]. The orange dashed line is evaluated by solving the Boltzmann equations of  $N_1$ ,  $\chi$  and  $\Delta L$  with  $Y_{N_2} = Y_{N_2}^{\text{eq}}$ . The dot-dashed dark red, dark green and dark blue lines are given by Eqs. (4.7), (4.14) and (4.15), respectively.

in the right panels. Roughly speaking, the relic of lepton asymmetry in the bottom line is given by that in the top line times the washout suppression factor.

In the case that the freeze-in production from  $N_2$  is dominant (top-left panel), we have to take the washout effect into account (for the detail, see Appendix C.2). The lepton asymmetry of this case is evaluated by

$$\mathcal{Y}_{\Delta L}^{\text{FI}}(z_1) = \int_0^{z_1} dx' \mathcal{F}_2(x') \exp \left[ - \int_{x'}^{z_1} dx'' W_2(x'') \right], \quad (4.7)$$

where

$$W_2 := \frac{1}{2Hx} \frac{K_1(m_{N_2}x/m_{N_1})}{K_2(m_{N_2}x/m_{N_1})} \left( \tilde{\Gamma}_2 + \Gamma_2 \frac{\mathbf{Y}_{\chi}}{Y_{\chi}^{\text{eq}}} \right) \frac{Y_{N_2}^{\text{eq}}}{Y_L^{\text{eq}}} + \frac{1}{2Hx} \frac{K_1(x)}{K_2(x)} \left( \tilde{\Gamma}_1 + \Gamma_1 \frac{\mathbf{Y}_{\chi}}{Y_{\chi}^{\text{eq}}} \right) \frac{Y_{N_2}^{\text{eq}}}{Y_L^{\text{eq}}}, \quad (4.8)$$

$$\mathcal{F}_2 = \frac{1}{Hx} \frac{K_1(m_{N_2}x/m_{N_1})}{K_2(m_{N_2}x/m_{N_1})} \Gamma_2 \epsilon_2 \left( \mathbf{Y}_{N_2} - \frac{Y_{N_2}^{\text{eq}}}{Y_{\chi}^{\text{eq}}} \mathbf{Y}_{\chi} \right) + \frac{1}{Hx} \frac{K_1(x)}{K_2(x)} \Gamma_1 \epsilon_1 \left( \mathbf{Y}_{N_1} - \frac{Y_{N_1}^{\text{eq}}}{Y_{\chi}^{\text{eq}}} \mathbf{Y}_{\chi} \right). \quad (4.9)$$

$$\mathbf{Y}_{N_2} = \frac{45\sqrt{10}}{2\pi^5 g_*^{1/2} g_*^S} \frac{M_P m_{N_2} \tilde{\Gamma}_2}{m_{N_1}^3} x^3, \quad (4.10)$$

$$\mathbf{Y}_\chi = \frac{135}{2\pi^6 g_* g_*^S} \frac{M_P^2 m_{N_2}^2 \tilde{\Gamma}_2 (\Gamma_{N_2 \rightarrow N_1 \chi} + \Gamma_2)}{m_{N_1}^6} x^6, \quad (4.11)$$

$$\mathbf{Y}_{N_1} = \frac{45\sqrt{10}}{2\pi^5 g_*^{1/2} g_*^S} \frac{M_P \tilde{\Gamma}_1}{m_{N_1}^2} x^3 + \frac{135}{2\pi^6 g_* g_*^S} \frac{M_P^2 m_{N_2}^2 \tilde{\Gamma}_2 (\Gamma_{N_2 \rightarrow N_1 \chi} + \Gamma_2)}{m_{N_1}^6} x^6. \quad (4.12)$$

$z_1$  is given by using these  $\mathbf{Y}_{N_2}$  and  $\mathbf{Y}_\chi$  as

$$z_1 = \min(z_{N_2}, z_\chi), \quad \mathbf{Y}_{N_2}(z_{N_2}) = \frac{45}{\pi^4 g_*^S}, \quad \mathbf{Y}_\chi(z_\chi) = \frac{45}{2\pi^4 g_*^S}, \quad (4.13)$$

and  $z_{N_2}$  ( $z_\chi$ ) is regarded as the time of  $N_2$  ( $\chi$ ) being close to the thermal equilibrium. The washout gives the exponential suppression through  $e^{-\int dx' W_2(x')}$ . On the other hand, if the  $N_1$  process is dominant, the asymmetry is mainly produced by the ordinary freeze-in mechanism via  $N_1$  decay such as the FIMP dark matter [19] (top-right panel in Fig. 5). The relic of the lepton asymmetry is written as

$$Y_{\Delta L}^{\text{FI}}(\infty) \approx \frac{135\sqrt{10}}{2\pi^5 g_*^{1/2} g_*^S} \frac{M_P \Gamma_1 \epsilon_1}{m_{N_1}^2} \int_0^\infty dx x^3 K_1(x) = \frac{405\sqrt{10}}{4\pi^4 g_*^{1/2} g_*^S} \frac{M_P \Gamma_1 \epsilon_1}{m_{N_1}^2}. \quad (4.14)$$

If the washout is strong and dilutes the relic from the  $N_1$  decay (bottom right panel in Fig. 5), the lepton asymmetry is evaluated as

$$\mathcal{Y}_{\Delta L}^{\text{WO}}(\infty) = \int_0^\infty dx' \mathcal{F}_1(x') \exp\left[-\int_{x'}^\infty dx'' W_1(x'')\right], \quad (4.15)$$

where the washout function of this case is given by

$$W_1 := \frac{1}{2Hx} \frac{K_1(m_{N_2}x/m_{N_1})}{K_2(m_{N_2}x/m_{N_1})} (\tilde{\Gamma}_2 + \Gamma_2) \frac{Y_{N_2}^{\text{eq}}}{Y_L^{\text{eq}}} + \frac{1}{2Hx} \frac{K_1(x)}{K_2(x)} (\tilde{\Gamma}_1 + \Gamma_1) \frac{Y_{N_1}^{\text{eq}}}{Y_L^{\text{eq}}}, \quad (4.16)$$

and we introduce the following function

$$\mathcal{F}_1 := \frac{1}{Hx} \frac{K_1(m_{N_2}x/m_{N_1})}{K_2(m_{N_2}x/m_{N_1})} \Gamma_2 \epsilon_2 \left(\frac{\tilde{\Gamma}_2 + \Gamma_2}{m_{N_2}}\right) Y_{N_2}^{\text{eq}} + \frac{1}{Hx} \frac{K_1(x)}{K_2(x)} \Gamma_1 \epsilon_1 \left(\frac{\tilde{\Gamma}_1 + \Gamma_1}{m_{N_1}}\right) Y_{N_1}^{\text{eq}}. \quad (4.17)$$

## 4.2 Parameter space

Based on the analysis of the Boltzmann equations in the previous subsection, we discuss the parameter spaces of the model where the lepton asymmetry is properly generated. The Majorana masses of the RH neutrinos are fixed to  $m_{N_1} = 10^{10}$  GeV,  $m_{N_2} = 10^{12}$  GeV, and  $m_{N_3} = 10^{14}$  GeV.  $N_3$  is heavy so that it is assumed not to join the initial and final states of our considering processes. The scalar  $\chi$  is light and its mass is assumed in this work to be  $m_\chi = 10^{-3}$  GeV, but its detailed value does not largely affect the asymmetry. As for the CI parameters (the degrees of freedom of neutrino Yukawa couplings), we consider the following two typical patterns of parameters:

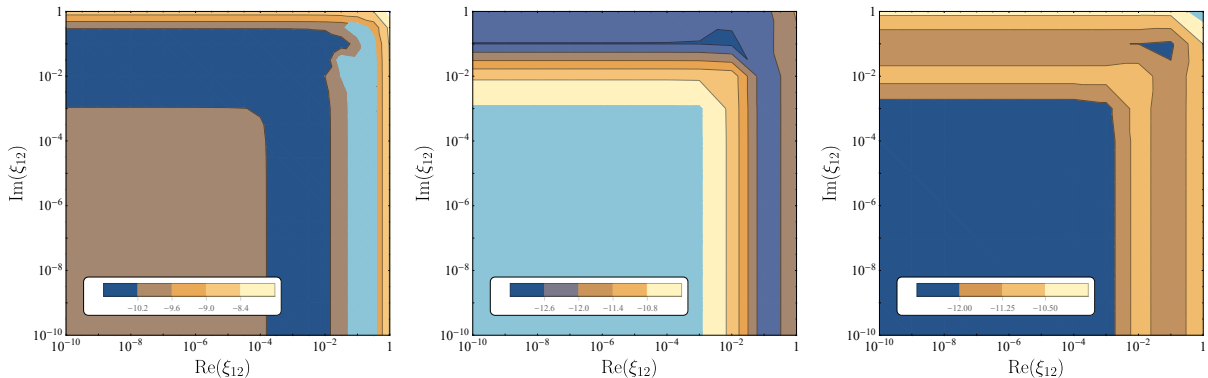


Figure 6: The density plots of the lepton asymmetry in the  $(\text{Re } \xi_{12}, \text{Im } \xi_{12})$  plane. The left panel is the parameter space for the normal mass hierarchy and all the CI parameters real-valued. In other two panels, the inverted mass hierarchy is assumed and the middle (right) panel shows the parameter space with all the CI parameters being real (pure imaginary). The light blue regions properly produce the observed baryon asymmetry in the Universe.

(I) Real CI parameters

$$\omega_{12} = \frac{1}{4}, \quad \omega_{23} = \frac{3}{7}, \quad \omega_{13} = 0 \quad (4.18)$$

(II) Pure imaginary CI parameters

$$\omega_{12} = 2i, \quad \omega_{23} = i, \quad \omega_{13} = 0. \quad (4.19)$$

With these parameter sets, the asymmetry from the SM particle loops vanish,  $\tilde{\epsilon}_i^{(LH)} = 0$ , found from Eq. (2.8).

Fig. 6 shows the relic of the lepton asymmetry  $Y_{\Delta L}(\infty)$  for

$$\text{Re } \xi = \begin{pmatrix} \frac{1}{20} & \text{Re } \xi_{12} \\ \text{Re } \xi_{12} & \frac{1}{10} \end{pmatrix}, \quad \text{Im } \xi = \begin{pmatrix} \frac{1}{2} & \text{Im } \xi_{12} \\ \text{Im } \xi_{12} & 1 \end{pmatrix}. \quad (4.20)$$

The light blue regions properly produce the observed baryon asymmetry. The CP asymmetry parameters Eqs. (3.7), (3.8) and (3.11)–(3.13) are roughly determined by the large values in  $\xi^2$ , which then lead to the contours seen in Fig. 6.

The left panel of Fig. 6 is the parameter space for the normal mass hierarchy of neutrinos and real CI parameters, where the washout effect is less dominant. In this case, larger values of couplings lead larger lepton asymmetry through the freeze-in like production of  $N_1$ . Then the lepton asymmetry reduces due to weaker couplings, but the asymmetry becomes large again when  $\xi_{12}$  is small enough. This is because the freeze-in like production of  $N_2$  is dominant. If the washout effect works well as in the inverted mass hierarchy, the lepton asymmetry is suppressed as shown in the middle and right panels of

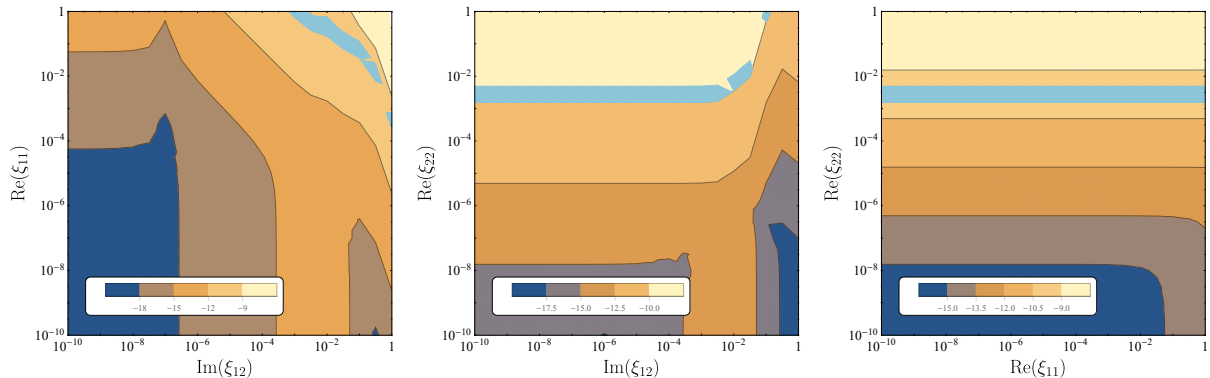


Figure 7: The density plots of the lepton asymmetry in the  $(\text{Im } \xi_{12}, \text{Re } \xi_{11})$ ,  $(\text{Im } \xi_{12}, \text{Re } \xi_{22})$  and  $(\text{Re } \xi_{11}, \text{Re } \xi_{22})$  planes with the parameterization (4.21). The normal mass hierarchy and real CI parameters are adopted for realizing  $Y_{\Delta L}(\infty) \sim 10^{-10}$ .

Fig. 6. When the CI parameters are real, the final value of the lepton asymmetry tends to converge to a value slightly smaller than  $10^{-10}$  if  $\xi$  are feeble couplings, which means the relic asymmetry is determined by the neutrino Yukawa couplings. However the washout is relatively stronger if  $\xi$  is larger, and the relic is more suppressed. On the other hand, the washout effect of neutrino Yukawa couplings works well and the lepton asymmetry can only take a tiny value. In this case, an enough large coupling is needed for a large amount of  $Y_{\Delta L}$  produced in the early Universe to explain the observed asymmetry even when it is washed out. From these observations, the tree-level leptogenesis from the three-body decay of RH neutrinos with a flavorful scalar does not favor the inverted mass hierarchy of neutrinos.

We now discuss a singlet scalar  $\chi$  and its general form of couplings to the RH neutrinos. If  $\chi$  is something like a pseudo-Nambu-Goldstone boson associated with the lepton number symmetry, the imaginary parts of the diagonal couplings  $\xi_{ii}$  tend to be dominant. Keeping in mind this fact, we take the coupling  $\xi$  as

$$\text{Re } \xi = \begin{pmatrix} \text{Re } \xi_{11} & 0 \\ 0 & \text{Re } \xi_{22} \end{pmatrix}, \quad \text{Im } \xi = \begin{pmatrix} 10^{-2} & \text{Im } \xi_{12} \\ \text{Im } \xi_{12} & 1 \end{pmatrix}. \quad (4.21)$$

The parameter spaces are shown in Fig. 7 when  $\text{Re } \xi_{11}$ ,  $\text{Re } \xi_{22}$  and  $\text{Im } \xi_{12}$  are assumed to be the modifications to the imaginary diagonal elements. In this situation, the lepton asymmetry is produced by the freeze-in mechanism of  $N_1$  or  $N_2$  as shown in the top panels of Fig. 5, and there exist the allowed regions between the parameter spaces of over- and under-productions of the asymmetry.

On the other hand, the parameter spaces of the imaginary diagonal elements are shown in Fig. 8. For evaluating the lepton asymmetry in these planes,  $\text{Im } \xi_{12}$  and one of  $\text{Im } \xi_{12}$  or  $\text{Re } \xi_{22}$  are fixed to  $10^{-1}$  or  $10^{-5}$ , and the normal mass hierarchy for the neutrino masses is assumed. As seen from these figures, larger couplings lead to larger relic asymmetry,

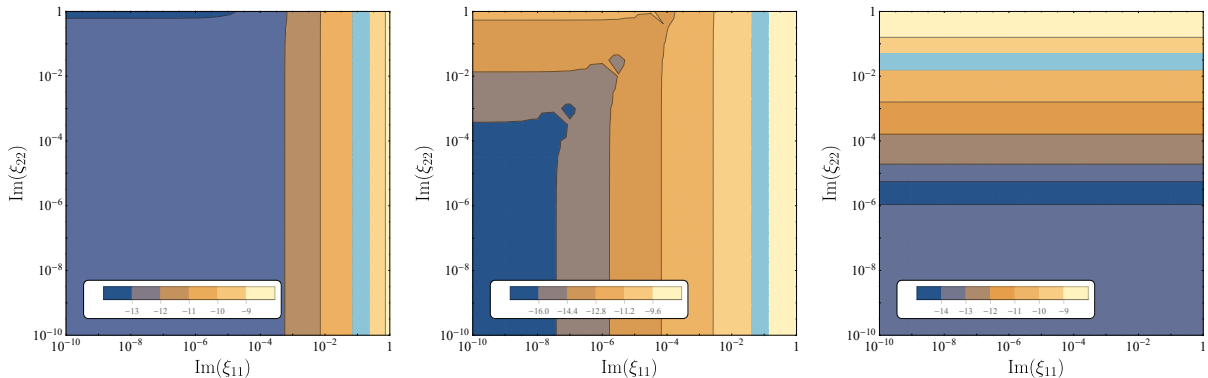


Figure 8: The density plots of the lepton asymmetry in the  $(\text{Im } \xi_{11}, \text{Im } \xi_{22})$  plane for the normal mass hierarchy. (Left)  $\text{Im } \xi_{12} = 10^{-1}$ ,  $\text{Re } \xi_{12} = 10^{-1}$ . (Middle)  $\text{Im } \xi_{12} = 10^{-5}$ ,  $\text{Re } \xi_{12} = 10^{-1}$ . (Right)  $\text{Im } \xi_{12} = 10^{-5}$ ,  $\text{Re } \xi_{22} = 10^{-1}$ .

similar to the above cases of the normal mass hierarchy, and  $\text{Im } \xi_{11}, \text{Im } \xi_{22} \sim 10^{-(1-2)}$  are favored.

### 4.3 Property of $\chi$ scalar

In the present work, the scalar field  $\chi$  has two important property that (i) it has the complex coupling  $\xi_{ij}$  to the parent decay particles and (ii) its remnant  $Y_\chi$  in the present Universe is large. That is a general result to have an appropriate order of baryon asymmetry generated from the three-body decay including  $\chi$ .

Let us first discuss about the coupling  $\xi_{ij}$ . The analysis in the above shows that  $\xi_{ij}$  should be complex-valued so that the CP asymmetry is properly produced through the three-body decay. Further the flavor-changing components  $\xi_{ij}$  ( $i \neq j$ ) can play an important role for the leptogenesis. These nature of couplings put some constraint on the property of the field  $\chi$ , for example, a dynamical completion in high-energy regime.

- Nambu-Goldstone boson :

A simple example for scalar couplings to neutrinos is the one whose vacuum expectation value (VEV) gives the masses of RH neutrinos  $N_i$ . If such a scalar is complex, the coupling has the lepton number symmetry (the chiral rotation of  $N_i$ ) and the scalar VEV breaks it. As a result of symmetry breaking, a Nambu-Goldstone boson (NGB) appears [20–22], which couples to  $N_i$  and can be identified to  $\chi$ . This is a typical and the simplest dynamical realization of the present model. It is however noticed that, if the NGB nature is exact,  $\chi$  is massless and its couplings to  $N_i$  are real and flavor diagonal, i.e.,  $\xi_{ij} = c_i \delta_{ij}$ ,  $c_i \in \mathbb{R}$ . As mentioned above, such a too simple form of scalar couplings is not suitable for generating the asymmetry.

- Flavor-dependent interaction :

There are several ways to ameliorate the NGB problem, too simple  $\xi_{ij}$ , found in



the above simplest setup. The first is to introduce multi scalars which couple to the RH neutrinos  $N_i$ . These scalars generally couple to each other and develop nonzero VEVs. The resultant NGB, which is identified to  $\chi$ , is a linear combination of (the phases of) these scalars. As a result, the flavor structure becomes different between the masses and the scalar couplings of RH neutrinos.

A more interesting realization is to assign generation-dependent charges to leptons under some flavor symmetry. The assignment is chosen so that the masses (and Yukawa couplings) are forbidden and then induced by some VEV of complex scalar, charged under the same flavor symmetry [23]. In this case,  $\chi$  is possibly the NGB of flavor symmetry and its coupling to leptons is determined by the flavor structure of lepton masses and symmetry charges. Unless the masses and charges have exactly the same structure, the  $\chi$  couplings are generally flavor dependent [24] (and complex valued). Typical examples may be constructed with flavor  $U(1)$  symmetry for fermion mass hierarchy, and non-universal anomaly-free lepton numbers such as  $L_\mu - L_\tau$  and others [25, 26].

- Radiative corrections :

The NGB property is not exactly hold if the original symmetry is somehow violated via explicit breaking terms. A well-known example is the scalar mass term which does not respect (global) symmetry, and hence the NGB acquires its nonzero mass (the “pion” mass) at classical level. With such explicit breaking, one generally expects to have non-vanishing radiative corrections to unusual NGB couplings and resolve the NGB problem mentioned above. There are phenomenological analysis for large breaking, e.g., a heavy NGB of the lepton number symmetry [27, 28], where suitably size of corrections might be obtained.

The large remnant of  $\chi$  is another characteristic result of the model. We here discuss two approaches to this issue: (i) additional scalar interactions. (ii) a very light  $\chi$ . The first resolution is to introduce additional interaction such that it suppresses the scalar abundance somewhere in the thermal history. However, when  $\chi$  is the NGB of high-scale symmetry, its large decay constant generally suppresses the  $\chi$  couplings to the SM fields and cannot give an enough suppression to the  $\chi$  abundance. For example, when  $\chi$  is the NGB of lepton number symmetry which couples to the RH neutrinos, a typical ratio  $\Gamma/H(T = m_\chi)$  is  $10^{-20} \xi^2 (m_\chi/\text{GeV})$ . We are therefore lead to the situation that the scalar including three-body decay is not a NGB-like pseudo-scalar  $\chi$  but some heavy real scalar  $\rho$  (heavier than the electroweak scale). As long as  $\rho$  is rather lighter than  $N_i$ , the analysis of leptogenesis from three-body decay discussed in this paper is unchanged even for  $N_i \rightarrow L_j H \rho$ . Dynamical examples of  $\rho$  are a partner of NGB (a radial fluctuation around a VEV), a massive scalar in the multi scalar scenario, and so on. A main difference between  $\chi$  and  $\rho$  is the interaction to other (SM) fields. In particular, for the Higgs portal interaction,  $\rho$  interacts with the portal quartic coupling  $\lambda$ , but  $\chi$  has a suppressed amplitude given by  $\lambda E^2/(\text{VEV})^2$  where  $E$  is the energy scale considered. Upon the decoupling  $E \sim m_\rho$  or  $m_\chi$ , the latter interaction (for  $\chi$ ) is too tiny to reduce

the abundance, and the former one (for  $\rho$ ) can be used for the suppression. Whether  $\rho$  is the dark matter component in the Universe or not depends on the model parameters, though both are possible to realize.

The second option is to assume that  $\chi$  is very light and does not contribute much to the mass density of the present Universe. The relic abundance of  $\chi$  is given by  $\Omega_\chi h^2 = m_\chi s_0 Y_{\chi,0}/(\varepsilon_{c,0}/h^2)$  with the today entropy and critical energy densities,  $s_0 = 2891 \text{ cm}^{-3}$  and  $\varepsilon_{c,0} = 5.16(h/0.7)^2 \text{ GeV/m}^3$ . If this abundance is required to be less than the observed dark matter density times a small ratio  $\delta$ , that implies the upper bound on  $m_\chi$ ,

$$m_\chi < \delta \frac{\Omega_{\text{DM}} \varepsilon_{c,0}}{s_0 Y_\chi^{\text{eq}}} = 1.89 \times 10^{-7} \delta \text{ [GeV]} \quad (4.22)$$

where we have assumed  $Y_{\chi,0}$  is equal to the equilibrium value  $Y_\chi^{\text{eq}}$ . For example,  $\chi$  has a sub-eV mass for  $\delta = 10^{-3}$  but weighs more than the current temperature. Furthermore the interaction of  $\chi$  to the SM sector is generally suppressed by  $\mathcal{O}(m_\nu)$ . Such a very light and feebly-interacting scalar may be harmlessly floating in the present Universe.

## 5 Summary

We have studied the lepton asymmetry produced by the tree-level RH neutrino three-body decays with a singlet scalar field. In order to cover the general case, we considered the scalar and pseudo-scalar couplings between the scalar field and RH neutrinos. We evaluated the RH neutrino two-body and three-body decay widths with the scalar field and the asymmetry parameters. For the decay widths, the  $k = l = 1$  contribution tends to be dominant in the lightest  $N_1$  decay, and the contribution of the resonant  $k = l = 1$  or the non-resonant  $k = l = 2$  is dominant depending on  $\xi$  in the heavier  $N_2$  decay. For the asymmetry parameters, not only usual cross terms but also the  $k = l = 1$  can be dominant to  $\epsilon_1$ , and the  $k = l = 2$  term is the leading contribution to  $\epsilon_2$ . In the latter two contributions, the CP asymmetry comes from a single decay process, which is characteristic of the existence of the flavorful scalar. We derived the Boltzmann equations and discussed there are four typical patterns of the lepton asymmetry production depending on the  $N_1$  or  $N_2$  decay process being dominant to the production and the washout effect being strong or weak. Based on these analysis, we show the parameter space of the model where the lepton asymmetry is properly generated. For example, we find the tree-level leptogenesis via the three-body decay with the flavorful scalar does not favor the inverted mass hierarchy due to the strong washout suppression, without a help of the two-body decay asymmetry.

In this paper, we consider a simplified model with a single flavorful scalar interacting to the RH neutrinos and investigate the possibility of the leptogenesis via the three-body decay with specific values of couplings. Pursuing the UV origin of this additional scalar such as a pseudo-Nambu-Goldstone boson and a more detailed analysis of flavor dynamics are important and left for future study.

## Acknowledgments

The authors thank to Takashi Toma and Takahiro Yoshida for useful comments and discussions. This work is supported by JSPS Grant-in-Aid for Scientific Research KAKENHI Grant No. JP20J11901 (YA), JP18H01214 and JP20K03949 (KY).

## A Three-body decay widths

We consider for simplicity the two-generation case  $N_{1,2}$ . The generalization to more generations is straightforward. We assume  $m_\chi \ll m_{N_i}$  and no large hierarchy among  $m_{N_i}$ . The masses of charged leptons and Higgs boson are dropped in the following formulae. The three-body decay width of the lightest RH neturino  $N_1$  is found from the full form (3.2) after the phase space integral as

$$\Gamma_{N_1 \rightarrow L_j H \chi} = \sum_{k,l} y_{1j}^\nu y_{kj}^{\nu*} \left( \xi_{1l}^* \xi_{1k} G_{kl}^A + \xi_{1l} \xi_{1k}^* G_{kl}^B + \xi_{1l}^* \xi_{1k} G_{kl}^C + \xi_{1l} \xi_{1k} G_{kl}^D \right) = \sum_{k,l} \Gamma_1^{(kl)}, \quad (\text{A.1})$$

where  $k, l$  indicate the contributions to the amplitudes which contain the intermediate states are  $N_{k,l}$ , respectively. For example,  $k \neq l$  means the cross term in the amplitude squared. Each piece  $G^{A,B,C,D}$  reads from the full form (3.2) and not explicitly given here. We instead show the exact form of  $\Gamma_1^{(kl)}$ , corresponding  $\mathcal{M}_k^* \mathcal{M}_l$ , where  $\mathcal{M}_m$  is the  $N_1$  three-body decay amplitude with the intermediate state  $N_m$ . The result is found in the limit of light  $m_\chi$  as

$$\Gamma_1^{(11)} = \frac{1}{128\pi^3} y_{1j}^\nu y_{1j}^{\nu*} \left[ |\xi_{11}|^2 m_{N_1} + \text{Re}(\xi_{11}^2 \bar{m}_{N_1}) \right] \ln \left( \frac{m_{N_1}}{m_\chi} \right), \quad (\text{A.2})$$

$$\begin{aligned} \Gamma_1^{(12)} = & \frac{1}{512\pi^3 m_{N_1}^3} y_{2j}^\nu y_{1j}^{\nu*} \left[ \xi_{11} \xi_{12}^* \bar{m}_{N_1} \bar{m}_{N_2}^* \left[ (m_{N_1}^2 + m_{N_2}^2) \ln \left( \frac{m_{N_2}^2}{m_{N_2}^2 - m_{N_1}^2} \right) - m_{N_1}^2 \right] \right. \\ & + 2m_{N_1} (\xi_{11} \xi_{12} \bar{m}_{N_1} + \xi_{11}^* \xi_{12}^* \bar{m}_{N_2}^*) \left[ m_{N_2}^2 \ln \left( \frac{m_{N_2}^2}{m_{N_2}^2 - m_{N_1}^2} \right) - m_{N_1}^2 \right] \\ & \left. + \xi_{11}^* \xi_{12} \left[ m_{N_2}^2 (m_{N_1}^2 + m_{N_2}^2) \ln \left( \frac{m_{N_2}^2}{m_{N_2}^2 - m_{N_1}^2} \right) - m_{N_1}^2 m_{N_2}^2 - \frac{3}{2} m_{N_1}^4 \right] \right], \quad (\text{A.3}) \end{aligned}$$

$$\Gamma_1^{(21)} = \Gamma_1^{(12)*}, \quad (\text{A.4})$$

$$\begin{aligned} \Gamma_1^{(22)} = & \frac{1}{512\pi^3 m_{N_1}^3} y_{2j}^\nu y_{2j}^{\nu*} \left[ |\xi_{12}|^2 \left[ (5m_{N_2}^4 - m_{N_1}^4) \ln \left( \frac{m_{N_2}^2}{m_{N_2}^2 - m_{N_1}^2} \right) - 5m_{N_1}^2 m_{N_2}^2 - \frac{5}{2} m_{N_1}^4 \right] \right. \\ & \left. + 4 \text{Re}(\xi_{12}^2 \bar{m}_{N_2}) m_{N_1} \left[ (2m_{N_2}^2 - m_{N_1}^2) \ln \left( \frac{m_{N_2}^2}{m_{N_2}^2 - m_{N_1}^2} \right) - 2m_{N_1}^2 \right] \right]. \quad (\text{A.5}) \end{aligned}$$

When  $N_2$  is much heavier than  $N_1$ , the expressions are reduced to

$$\Gamma_1^{(12)} = \Gamma_1^{(21)*} \approx \frac{m_{N_1} \bar{m}_{N_2}^*}{1024\pi^3 m_{N_2}^2} y_{2j}^\nu y_{1j}^{\nu*} \xi_{12}^* (3\xi_{11} \bar{m}_{N_1} + 2\xi_{11}^* m_{N_1}), \quad (\text{A.6})$$

$$\Gamma_1^{(22)} \approx \frac{m_{N_1}^3}{768\pi^3 m_{N_2}^2} y_{2j}^\nu y_{2j}^{\nu*} |\xi_{12}|^2. \quad (\text{A.7})$$

The last equation implies that the  $k = l = 2$  mode does not induce CP asymmetry at the leading order and then highly suppressed for the  $N_1$  decay.

For a heavier RH neutrino, its three-body decay can meet the resonance around the mass of a lighter intermediate state, and then the width is largely enhanced. In the present case, the  $N_2$  decay width  $\Gamma_{N_2 \rightarrow L_j H \chi}$  has the enhancement both for  $k = l = 1$  and the sum of cross terms, namely,  $\Gamma_2^{(11)}$  and  $\Gamma_2^{(12)} + \Gamma_2^{(21)}$  in the similar notation as (A.1). These on-shell contributions to the decay width are evaluated from the full form (3.2) with the narrow width approximation. For the  $k = l = 1$  part, we obtain

$$\Gamma_2^{(11)} = \frac{m_{N_1}}{256\pi^2} \frac{m_{N_2}^2 - m_{N_1}^2}{m_{N_2}^3 \Gamma_{N_1}} y_{1j}^\nu y_{1j}^{\nu*} \left[ |\xi_{12}|^2 (m_{N_1}^2 + m_{N_2}^2) + 2 \text{Re}(\xi_{12}^2 \bar{m}_{N_1}) m_{N_2} \right], \quad (\text{A.8})$$

where  $\Gamma_{N_1}$  in the denominator indicates  $N_1$  is the real intermediate state. Compared with the decay width for  $N_2 \rightarrow N_1 \chi$  given in (2.6), the on-shell  $k = l = 1$  contribution is found

$$\Gamma_2^{(11)} \approx \frac{m_{N_1}}{16\pi \Gamma_{N_1}} y_{1j}^\nu y_{1j}^{\nu*} \Gamma_{N_2 \rightarrow N_1 \chi} \approx \frac{1}{2} \Gamma_{N_2 \rightarrow N_1 \chi}. \quad (\text{A.9})$$

For the cross-term part, a similar evaluation leads to the on-shell resonant contribution,

$$\begin{aligned} \Gamma_2^{(12)} + \Gamma_2^{(21)} = & \frac{m_{N_1}}{256\pi^2 m_{N_2}^3 (m_{N_2}^2 - m_{N_1}^2)} \left[ \Gamma_{N_2} \left[ \frac{1}{2} \text{Re}(y_{2j}^\nu y_{1j}^{\nu*} \xi_{22}^* \xi_{12}) (m_{N_1}^2 + m_{N_2}^2)^2 \right. \right. \\ & - 4 \text{Im}(y_{2j}^\nu y_{1j}^{\nu*} \xi_{12}^*) \text{Im}(\xi_{22}) m_{N_1} m_{N_2} (m_{N_1}^2 + m_{N_2}^2) + 2 \text{Re}(y_{2j}^\nu y_{1j}^{\nu*} \xi_{22} \xi_{12}) m_{N_1}^2 m_{N_2}^2 \left. \right] \\ & - \left[ \text{Im}(y_{2j}^\nu y_{1j}^{\nu*} \xi_{22} \xi_{12}^*) m_{N_1} + \text{Im}(y_{2j}^\nu y_{1j}^{\nu*} \xi_{22}^* \xi_{12}) m_{N_2} \right] (m_{N_2}^4 - m_{N_1}^4) \\ & - 2 \left[ \text{Im}(y_{2j}^\nu y_{1j}^{\nu*} \xi_{22} \xi_{12}) m_{N_1} + \text{Im}(y_{2j}^\nu y_{1j}^{\nu*} \xi_{22}^* \xi_{12}^*) m_{N_2} \right] m_{N_1} m_{N_2} (m_{N_2}^2 - m_{N_1}^2) \left. \right]. \end{aligned} \quad (\text{A.10})$$

Finally the non-resonant part,  $k = l = 2$ , gives

$$\Gamma_2^{(22)} = \frac{1}{128\pi^3} y_{2j}^\nu y_{2j}^{\nu*} \left[ |\xi_{22}|^2 m_{N_2} + \text{Re}(\xi_{22}^2 \bar{m}_{N_2}) \right] \ln \left( \frac{m_{N_2}}{m_\chi} \right). \quad (\text{A.11})$$

## B CP asymmetry (width differences)

For a real particle (a real scalar, a Majorana fermion, etc), the decay to anti-particle final states is obtained by replacing all coupling constants with their complex conjugates in the corresponding decay amplitude to particle final states. In the present case, the three-body decay of  $N_i$  to the anti-lepton  $\bar{L}_j$ , the conjugate of Higgs boson  $\bar{H}$ , and the real scalar  $\chi$  is described by  $y^\nu \leftrightarrow y^{\nu*}$  and  $\xi \leftrightarrow \xi^*$  (and  $P_R \leftrightarrow P_L$ ) everywhere in the amplitude. The CP asymmetry is induced at the decay, proportionally to the difference of decay widths to

particles and corresponding anti-particles. As a result, the asymmetry is originated from the pieces in the decay widths which are not real with respect to coupling constants.

The decay width to anti-particles is defined in a similar way to the decay to particles discussed in the previous section, namely,

$$\Gamma_{N_1 \rightarrow L_j^c H^\dagger \chi} = \sum_{k,l} \bar{\Gamma}_1^{(kl)}. \quad (\text{B.1})$$

The differences of partial widths are written as  $\Delta\Gamma_1^{(kl)} = \Gamma_1^{(kl)} - \bar{\Gamma}_1^{(kl)}$ . From the explicit forms for  $\Gamma_1^{(kl)}$  and the replacement rule mentioned above, we obtain

$$\Delta\Gamma_1^{(11)} = \frac{\Gamma_{N_1}}{128\pi^3} y_{1j}^\nu y_{1j}^{\nu*} \text{Im}(\xi_{11}^2) \ln\left(\frac{m_{N_1}}{m_\chi}\right), \quad (\text{B.2})$$

$$\begin{aligned} \Delta\Gamma_1^{(12)} + \Delta\Gamma_1^{(21)} &= \frac{1}{256\pi^3 m_{N_1}^3} \left[ \text{Im}(y_{2j}^\nu y_{1j}^{\nu*} \xi_{11} \xi_{12}^*) (\Gamma_{N_1} m_{N_2} - \Gamma_{N_2} m_{N_1}) \right. \\ &\quad \times \left[ \left( m_{N_1}^2 + m_{N_2}^2 \right) \ln\left(\frac{m_{N_2}^2}{m_{N_2}^2 - m_{N_1}^2}\right) - m_{N_1}^2 \right] \\ &\quad + m_{N_1} \left[ \text{Im}(y_{2j}^\nu y_{1j}^{\nu*} \xi_{11} \xi_{12}) \Gamma_{N_1} - \text{Im}(y_{2j}^\nu y_{1j}^{\nu*} \xi_{11}^* \xi_{12}^*) \Gamma_{N_2} \right] \\ &\quad \left. \times \left[ m_{N_2}^2 \ln\left(\frac{m_{N_2}^2}{m_{N_2}^2 - m_{N_1}^2}\right) - m_{N_1}^2 \right] \right], \quad (\text{B.3}) \end{aligned}$$

$$\Delta\Gamma_1^{(22)} = \frac{\Gamma_{N_2}}{128\pi^3 m_{N_1}^2} y_{2j}^\nu y_{2j}^{\nu*} \text{Im}(\xi_{12}^2) \left[ (2m_{N_2}^2 - m_{N_1}^2) \ln\left(\frac{m_{N_2}^2}{m_{N_2}^2 - m_{N_1}^2}\right) - 2m_{N_1}^2 \right]. \quad (\text{B.4})$$

When  $N_2$  is much heavier than  $N_1$ , the expressions are reduced to

$$\Delta\Gamma_1^{(12)} + \Delta\Gamma_1^{(21)} \approx \frac{-m_{N_1}^2 \Gamma_{N_2}}{512\pi^3 m_{N_2}^2} \text{Im} \left[ y_{2j}^\nu y_{1j}^{\nu*} \xi_{12}^* (3\xi_{11} + 2\xi_{11}^*) \right], \quad (\text{B.5})$$

$$\Delta\Gamma_1^{(22)} \approx \frac{m_{N_1}^4 \Gamma_{N_2}}{768\pi^3 m_{N_2}^4} y_{2j}^\nu y_{2j}^{\nu*} \text{Im}(\xi_{12}^2). \quad (\text{B.6})$$

In a similar way, we have the width differences for the  $N_2$  resonant and non-resonant three-body decay,

$$\Delta\Gamma_2^{(11)} = \frac{m_{N_1}}{128\pi^2} \frac{m_{N_2}^2 - m_{N_1}^2}{m_{N_2}^2} y_{1j}^\nu y_{1j}^{\nu*} \text{Im}(\xi_{12}^2), \quad (\text{B.7})$$

$$\begin{aligned} \Delta\Gamma_2^{(12)} + \Delta\Gamma_2^{(21)} &= \frac{-m_{N_1}}{128\pi^2 m_{N_2}^3} \left[ \left[ \text{Im}(y_{2j}^\nu y_{1j}^{\nu*} \xi_{22} \xi_{12}^*) m_{N_1} + \text{Im}(y_{2j}^\nu y_{1j}^{\nu*} \xi_{22}^* \xi_{12}) m_{N_2} \right] (m_{N_1}^2 + m_{N_2}^2) \right. \\ &\quad \left. + 2 \left[ \text{Im}(y_{2j}^\nu y_{1j}^{\nu*} \xi_{22} \xi_{12}) m_{N_1} + \text{Im}(y_{2j}^\nu y_{1j}^{\nu*} \xi_{22}^* \xi_{12}^*) m_{N_2} \right] m_{N_1} m_{N_2} \right], \quad (\text{B.8}) \end{aligned}$$

$$\Delta\Gamma_2^{(22)} = \frac{\Gamma_{N_2}}{128\pi^3} y_{2j}^\nu y_{2j}^{\nu*} \text{Im}(\xi_{22}^2) \ln\left(\frac{m_{N_2}}{m_\chi}\right). \quad (\text{B.9})$$

# C Boltzmann equations and asymmetry formulae

## C.1 Boltzmann equations

The Boltzmann equations for the system of Eq. (2.1) are given by

$$\begin{aligned}
Hx \frac{dY_{N_1}}{dx} &= \frac{K_1(m_{N_1}/T)}{K_2(m_{N_1}/T)} Y_{N_1}^{\text{eq}} \left[ \sum_j \tilde{\Gamma}_{1j} \left( 1 - \frac{Y_{N_1}}{Y_{N_1}^{\text{eq}}} \right) - \frac{1}{2} \sum_j \tilde{\Gamma}_{1j} \tilde{\epsilon}_{1j} \frac{Y_{\Delta L_j}}{Y_L^{\text{eq}}} \right. \\
&\quad \left. + \sum_j \Gamma_{1j} \left( \frac{Y_\chi}{Y_\chi^{\text{eq}}} - \frac{Y_{N_1}}{Y_{N_1}^{\text{eq}}} \right) - \frac{1}{2} \sum_j \Gamma_{1j} \epsilon_{1j} \frac{Y_\chi}{Y_\chi^{\text{eq}}} \frac{Y_{\Delta L_j}}{Y_L^{\text{eq}}} \right] \\
&\quad + \frac{K_1(m_{N_2}/T)}{K_2(m_{N_2}/T)} Y_{N_2}^{\text{eq}} \Gamma_{N_2 \rightarrow N_1 \chi} \left( \frac{Y_{N_2}}{Y_{N_2}^{\text{eq}}} - \frac{Y_{N_1}}{Y_{N_1}^{\text{eq}}} \frac{Y_\chi}{Y_\chi^{\text{eq}}} \right) + C_{\text{scat.}}, \tag{C.1}
\end{aligned}$$

$$\begin{aligned}
Hx \frac{dY_{N_2}}{dx} &= \frac{K_1(m_{N_2}/T)}{K_2(m_{N_2}/T)} Y_{N_2}^{\text{eq}} \left[ \sum_j \tilde{\Gamma}_{2j} \left( 1 - \frac{Y_{N_2}}{Y_{N_2}^{\text{eq}}} \right) - \frac{1}{2} \sum_j \tilde{\Gamma}_{2j} \tilde{\epsilon}_{2j} \frac{Y_{\Delta L_j}}{Y_L^{\text{eq}}} \right. \\
&\quad \left. + \sum_j \Gamma_{2j} \left( \frac{Y_\chi}{Y_\chi^{\text{eq}}} - \frac{Y_{N_2}}{Y_{N_2}^{\text{eq}}} \right) - \frac{1}{2} \sum_j \Gamma_{2j} \epsilon_{2j} \frac{Y_\chi}{Y_\chi^{\text{eq}}} \frac{Y_{\Delta L_j}}{Y_L^{\text{eq}}} \right. \\
&\quad \left. - \Gamma_{N_2 \rightarrow N_1 \chi} \left( \frac{Y_{N_2}}{Y_{N_2}^{\text{eq}}} - \frac{Y_{N_1}}{Y_{N_1}^{\text{eq}}} \frac{Y_\chi}{Y_\chi^{\text{eq}}} \right) \right] + C_{\text{scat.}}, \tag{C.2}
\end{aligned}$$

$$\begin{aligned}
Hx \frac{dY_{\Delta L_i}}{dx} &= \sum_j \frac{K_1(m_{N_j}/T)}{K_2(m_{N_j}/T)} Y_{N_j}^{\text{eq}} \left[ \tilde{\Gamma}_{ji} \tilde{\epsilon}_{ji} \left( \frac{Y_{N_j}}{Y_{N_j}^{\text{eq}}} - 1 \right) - \frac{1}{2} \tilde{\Gamma}_{ji} \frac{Y_{\Delta L_i}}{Y_L^{\text{eq}}} \right. \\
&\quad \left. + \Gamma_{ji} \epsilon_{ji} \left( \frac{Y_{N_j}}{Y_{N_j}^{\text{eq}}} - \frac{Y_\chi}{Y_\chi^{\text{eq}}} \right) - \frac{1}{2} \Gamma_{ji} \frac{Y_\chi}{Y_\chi^{\text{eq}}} \frac{Y_{\Delta L_j}}{Y_L^{\text{eq}}} \right] \\
&\quad + C_{\text{scat.}}, \tag{C.3}
\end{aligned}$$

$$\begin{aligned}
Hx \frac{dY_\chi}{dx} &= \sum_{i,j} \frac{K_1(m_{N_i}/T)}{K_2(m_{N_i}/T)} Y_{N_i}^{\text{eq}} \left[ \Gamma_{ij} \left( \frac{Y_{N_i}}{Y_{N_i}^{\text{eq}}} - \frac{Y_\chi}{Y_\chi^{\text{eq}}} \right) + \frac{1}{2} \Gamma_{ij} \epsilon_{ij} \frac{Y_\chi}{Y_\chi^{\text{eq}}} \frac{Y_{\Delta L}}{Y_L^{\text{eq}}} \right] \\
&\quad + \frac{K_1(m_{N_2}/T)}{K_2(m_{N_2}/T)} Y_{N_2}^{\text{eq}} \Gamma_{N_2 \rightarrow N_1 \chi} \left( \frac{Y_{N_2}}{Y_{N_2}^{\text{eq}}} - \frac{Y_{N_1}}{Y_{N_1}^{\text{eq}}} \frac{Y_\chi}{Y_\chi^{\text{eq}}} \right) + C_{\text{scat.}}. \tag{C.4}
\end{aligned}$$

$C_{\text{scat.}}$  denotes the collision terms of the scattering divided by the entropy density with the on-shell contribution removed. In deriving these equations, the SM particles, in particular the leptons and the Higgs bosons, are assumed to be in thermal equilibrium:

$$Y_{L_j} = Y_L^{\text{eq}} + \frac{1}{2} Y_{\Delta L_j}, \quad Y_{\bar{L}_j} = Y_L^{\text{eq}} - \frac{1}{2} Y_{\Delta L_j}, \quad Y_H = Y_{\bar{H}} = Y_H^{\text{eq}}, \tag{C.5}$$

with the lepton asymmetry of  $j$ -th generation  $Y_{\Delta L_j}$ . In this paper, we analyze the Boltzmann equations with the single-flavored approximation. The total lepton asymmetry is defined by

$$Y_{\Delta L} := \sum_i Y_{\Delta L_i}, \tag{C.6}$$

and the collision terms are approximated as in the following forms:

$$\sum_i \Gamma_{ji} \frac{Y_{\Delta L_i}}{Y_{L_i}^{\text{eq}}} \sim \Gamma_j \frac{Y_{\Delta L}}{Y_L^{\text{eq}}}, \quad \sum_i \Gamma_{ji} \tilde{\epsilon}_{ji} \frac{Y_{\Delta L_i}}{Y_{L_i}^{\text{eq}}} \sim \Gamma_j \epsilon_j \frac{Y_{\Delta L}}{Y_L^{\text{eq}}}, \quad (\text{C.7})$$

$$\sum_i \tilde{\Gamma}_{ji} \frac{Y_{\Delta L_i}}{Y_{L_i}^{\text{eq}}} \sim \tilde{\Gamma}_j \frac{Y_{\Delta L}}{Y_L^{\text{eq}}}, \quad \sum_i \tilde{\Gamma}_{ji} \tilde{\epsilon}_{ji} \frac{Y_{\Delta L_i}}{Y_{L_i}^{\text{eq}}} \sim \tilde{\Gamma}_j \tilde{\epsilon}_j \frac{Y_{\Delta L}}{Y_L^{\text{eq}}}. \quad (\text{C.8})$$

Using these equations, the Boltzmann equations (C.1)–(C.4) are rewritten as

$$\begin{aligned} Hx \frac{dY_{N_1}}{dx} \approx & \frac{K_1(m_{N_1}/T)}{K_2(m_{N_1}/T)} Y_{N_1}^{\text{eq}} \left[ \tilde{\Gamma}_1 \left( 1 - \frac{Y_{N_1}}{Y_{N_1}^{\text{eq}}} \right) - \frac{1}{2} \tilde{\Gamma}_1 \tilde{\epsilon}_1 \frac{Y_{\Delta L}}{Y_L^{\text{eq}}} + \Gamma_1 \left( -\frac{Y_{N_1}}{Y_{N_1}^{\text{eq}}} + \frac{Y_\chi}{Y_\chi^{\text{eq}}} \right) \right. \\ & \left. - \frac{1}{2} \Gamma_1 \epsilon_1 \frac{Y_\chi}{Y_\chi^{\text{eq}}} \frac{Y_{\Delta L}}{Y_L^{\text{eq}}} \right] + \frac{K_1(m_{N_2}/T)}{K_2(m_{N_2}/T)} Y_{N_2}^{\text{eq}} \Gamma_{N_2 \rightarrow N_1 \chi} \left( \frac{Y_{N_2}}{Y_{N_2}^{\text{eq}}} - \frac{Y_{N_1}}{Y_{N_1}^{\text{eq}}} \frac{Y_\chi}{Y_\chi^{\text{eq}}} \right) + C_{\text{scat.}}, \end{aligned} \quad (\text{4.3})$$

$$\begin{aligned} Hx \frac{dY_{N_2}}{dx} \approx & \frac{K_1(m_{N_2}/T)}{K_2(m_{N_2}/T)} Y_{N_2}^{\text{eq}} \left[ \tilde{\Gamma}_2 \left( 1 - \frac{Y_{N_2}}{Y_{N_2}^{\text{eq}}} \right) - \frac{1}{2} \tilde{\Gamma}_2 \tilde{\epsilon}_2 \frac{Y_{\Delta L}}{Y_L^{\text{eq}}} + \Gamma_2 \left( -\frac{Y_{N_2}}{Y_{N_2}^{\text{eq}}} + \frac{Y_\chi}{Y_\chi^{\text{eq}}} \right) \right. \\ & \left. - \frac{1}{2} \Gamma_2 \epsilon_2 \frac{Y_\chi}{Y_\chi^{\text{eq}}} \frac{Y_{\Delta L}}{Y_L^{\text{eq}}} - \Gamma_{N_2 \rightarrow N_1 \chi} \left( \frac{Y_{N_2}}{Y_{N_2}^{\text{eq}}} - \frac{Y_{N_1}}{Y_{N_1}^{\text{eq}}} \frac{Y_\chi}{Y_\chi^{\text{eq}}} \right) \right] + C_{\text{scat.}}, \end{aligned} \quad (\text{4.4})$$

$$\begin{aligned} Hx \frac{dY_{\Delta L}}{dx} \approx & \sum_i \frac{K_1(m_{N_i}/T)}{K_2(m_{N_i}/T)} Y_{N_i}^{\text{eq}} \left[ \tilde{\Gamma}_i \tilde{\epsilon}_i \left( \frac{Y_{N_i}}{Y_{N_i}^{\text{eq}}} - 1 \right) - \frac{1}{2} \tilde{\Gamma}_i \frac{Y_{\Delta L}}{Y_L^{\text{eq}}} \right. \\ & \left. + \Gamma_i \epsilon_i \left( \frac{Y_{N_i}}{Y_{N_i}^{\text{eq}}} - \frac{Y_\chi}{Y_\chi^{\text{eq}}} \right) - \frac{1}{2} \Gamma_i \frac{Y_\chi}{Y_\chi^{\text{eq}}} \frac{Y_{\Delta L}}{Y_L^{\text{eq}}} \right] + C_{\text{scat.}}, \end{aligned} \quad (\text{4.5})$$

$$\begin{aligned} Hx \frac{dY_\chi}{dx} \approx & \sum_i \frac{K_1(m_{N_i}/T)}{K_2(m_{N_i}/T)} Y_{N_i}^{\text{eq}} \left[ \Gamma_i \left( \frac{Y_{N_i}}{Y_{N_i}^{\text{eq}}} - \frac{Y_\chi}{Y_\chi^{\text{eq}}} \right) + \frac{1}{2} \Gamma_i \epsilon_i \frac{Y_\chi}{Y_\chi^{\text{eq}}} \frac{Y_{\Delta L}}{Y_L^{\text{eq}}} \right] \\ & + Y_{N_2}^{\text{eq}} \frac{K_1(m_{N_2}/T)}{K_2(m_{N_2}/T)} \Gamma_{N_2 \rightarrow N_1 \chi} \left( \frac{Y_{N_2}}{Y_{N_2}^{\text{eq}}} - \frac{Y_{N_1}}{Y_{N_1}^{\text{eq}}} \frac{Y_\chi}{Y_\chi^{\text{eq}}} \right) + C_{\text{scat.}} \end{aligned} \quad (\text{4.6})$$

## C.2 Phenomenological formulae for lepton asymmetry

The Boltzmann equation of the lepton asymmetry (e.g. Eq. (4.5)) has following form:

$$\frac{dY_{\Delta L}(x)}{dx} = \mathcal{F}(x) - W(x)Y_{\Delta L}(x), \quad (\text{C.9})$$

where  $\mathcal{F}(x)$  is the  $Y_{\Delta L}$  independent function describing the asymmetry production from decays and scatterings of  $N_i$  and  $W(x)$  is the washout function. As discussed in Refs. [16, 29, 30], the solution of this equation can be expressed by

$$Y_{\Delta L}(x) = \int_{x_i}^x dx' \mathcal{F}(x') \exp \left[ - \int_{x'}^x dx'' W(x'') \right] + Y_{\Delta L}(x_i) \exp \left[ - \int_{x_i}^x dx'' W(x'') \right]. \quad (\text{C.10})$$

Intuitively, the integral of  $\mathcal{F}$  means the freeze-in like production [19] and  $e^{-\int dx' W(x')}$  denotes the washout suppression. Using this equation, we will show the approximated values of the lepton asymmetry,  $\mathcal{Y}_{\Delta L}^{\text{FI}}(z_1)$  and  $\mathcal{Y}_{\Delta L}^{\text{WO}}(\infty)$  in the following part of this section.

### C.2.1 Case for freeze-in from $N_2$

$N_2$  is mainly produced by the first term of the RHS in Eq. (4.4). Using the approximation for the modified Bessel function

$$K_n(x) \underset{x \sim 0}{\sim} \frac{(n-1)!}{2} \left(\frac{x}{2}\right)^{-n}, \quad (\text{C.11})$$

the Boltzmann equation is approximately written as

$$\frac{dY_{N_2}}{dx} \approx \frac{1}{Hx} \frac{K_1\left(\frac{m_{N_2}}{m_{N_1}}x\right)}{K_2\left(\frac{m_{N_2}}{m_{N_1}}x\right)} \tilde{\Gamma}_2 Y_{N_2}^{\text{eq}} \sim \frac{135\sqrt{10}}{2\pi^5 g_*^{1/2} g_*^S} \frac{M_P m_{N_2} \tilde{\Gamma}_2}{m_{N_1}^3} x^2, \quad (\text{C.12})$$

and the yield of  $N_2$  is scaled by

$$\mathbf{Y}_{N_2} = \frac{45\sqrt{10}}{2\pi^5 g_*^{1/2} g_*^S} \frac{M_P m_{N_2} \tilde{\Gamma}_2}{m_{N_1}^3} x^3. \quad (\text{C.13})$$

This  $N_2$  produces  $\chi$  and  $N_1$  via  $N_2 \rightarrow N_1 \chi$  process, and their yields are also written as

$$\mathbf{Y}_\chi = \frac{135}{2\pi^6 g_* g_*^S} \frac{M_P^2 m_{N_2}^2 \tilde{\Gamma}_2 (\Gamma_{N_2 \rightarrow N_1 \chi} + \Gamma_2)}{m_{N_1}^6} x^6, \quad (\text{C.14})$$

$$\mathbf{Y}_{N_1} = \frac{45\sqrt{10}}{2\pi^5 g_*^{1/2} g_*^S} \frac{M_P \tilde{\Gamma}_1}{m_{N_1}^2} x^3 + \frac{135}{2\pi^6 g_* g_*^S} \frac{M_P^2 m_{N_2}^2 \tilde{\Gamma}_2 (\Gamma_{N_2 \rightarrow N_1 \chi} + \Gamma_2)}{m_{N_1}^6} x^6. \quad (\text{C.15})$$

where the contribution of the first term of the RHS in Eq. (4.3) is included, which is scaled by  $x^3$  as in the same way to  $N_2$ . Using these functions, we will evaluate the lepton asymmetry. From Eq. (4.5), The washout function

$$W_2 := \frac{1}{2Hx} \frac{K_1(m_{N_2}x/m_{N_1})}{K_2(m_{N_2}x/m_{N_1})} \left( \tilde{\Gamma}_2 + \Gamma_2 \frac{\mathbf{Y}_\chi}{Y_\chi^{\text{eq}}} \right) \frac{Y_{N_2}^{\text{eq}}}{Y_L^{\text{eq}}} + \frac{1}{2Hx} \frac{K_1(x)}{K_2(x)} \left( \tilde{\Gamma}_1 + \Gamma_1 \frac{\mathbf{Y}_\chi}{Y_\chi^{\text{eq}}} \right) \frac{Y_{N_2}^{\text{eq}}}{Y_L^{\text{eq}}}, \quad (\text{C.16})$$

is read, and the yield is evaluated by using (C.10) as

$$\mathcal{Y}_{\Delta L}^{\text{FI}}(x) = \int_0^x dx' \mathcal{F}_2(x') \exp\left[-\int_{x'}^x dx'' W_2(x'')\right], \quad (\text{C.17})$$

with

$$\mathcal{F}_2 = \frac{1}{Hx} \frac{K_1(m_{N_2}x/m_{N_1})}{K_2(m_{N_2}x/m_{N_1})} \Gamma_2 \epsilon_2 \left( \mathbf{Y}_{N_2} - \frac{Y_{N_2}^{\text{eq}}}{Y_\chi^{\text{eq}}} \mathbf{Y}_\chi \right) + \frac{1}{Hx} \frac{K_1(x)}{K_2(x)} \Gamma_1 \epsilon_1 \left( \mathbf{Y}_{N_1} - \frac{Y_{N_1}^{\text{eq}}}{Y_\chi^{\text{eq}}} \mathbf{Y}_\chi \right). \quad (\text{C.18})$$

If the washout suppression is weak enough, which is the case of the neutrino Yukawa couplings being small, the lepton asymmetry is mainly produced by the RH neutrinos before getting into the thermal bath and the total amount is evaluated as

$$Y_{\Delta L} \approx \mathcal{Y}_{\Delta L}^{\text{FI}}(z_1), \quad (\text{C.19})$$



where

$$z_1 = \min(z_{N_2}, z_\chi), \quad \mathbf{Y}_{N_2}(z_{N_2}) = \frac{45}{\pi^4 g_*^S}, \quad \mathbf{Y}_\chi(z_\chi) = \frac{45}{2\pi^4 g_*^S}. \quad (\text{C.20})$$

This is regarded as the asymmetry by the freeze-in production including the weak washout effects.

### C.2.2 Case for strong $N_1$ washout

If the washout of  $N_1$  is strong, the lepton asymmetry is mainly determined by this, and the contribution from  $\mathcal{Y}_{\Delta L}^{\text{FI}}(z_1)$  is exponentially suppressed. The washout function of this case is given by

$$W_1 := \frac{1}{2Hx} \frac{K_1(m_{N_2}x/m_{N_1})}{K_2(m_{N_2}x/m_{N_1})} (\tilde{\Gamma}_2 + \Gamma_2) \frac{Y_{N_2}^{\text{eq}}}{Y_L^{\text{eq}}} + \frac{1}{2Hx} \frac{K_1(x)}{K_2(x)} (\tilde{\Gamma}_1 + \Gamma_1) \frac{Y_{N_1}^{\text{eq}}}{Y_L^{\text{eq}}}, \quad (\text{C.21})$$

where  $Y_\chi \approx Y_\chi^{\text{eq}}$  is assumed. Then, the lepton asymmetry is written as

$$\mathcal{Y}_{\Delta L}^{\text{WO}} = \int_0^x dx' \mathcal{F}_1(x') \exp\left[-\int_{x'}^x dx'' W_1(x'')\right], \quad (\text{C.22})$$

where we introduce the following function

$$\mathcal{F}_1 := \frac{1}{Hx} \frac{K_1(m_{N_2}x/m_{N_1})}{K_2(m_{N_2}x/m_{N_1})} \Gamma_2 \epsilon_2 \left(\frac{\tilde{\Gamma}_2 + \Gamma_2}{m_{N_2}}\right) Y_{N_2}^{\text{eq}} + \frac{1}{Hx} \frac{K_1(x)}{K_2(x)} \Gamma_1 \epsilon_1 \left(\frac{\tilde{\Gamma}_1 + \Gamma_1}{m_{N_1}}\right) Y_{N_1}^{\text{eq}}. \quad (\text{C.23})$$

Using these functions, the lepton asymmetry is given by

$$Y_{\Delta L} \approx \mathcal{Y}_{\Delta L}^{\text{WO}}(\infty). \quad (\text{C.24})$$

## References

- [1] P. Minkowski,  $\mu \rightarrow e\gamma$  at a Rate of One Out of  $10^9$  Muon Decays?, *Phys. Lett. B* **67** (1977) 421–428.
- [2] T. Yanagida, *Horizontal gauge symmetry and masses of neutrinos*, Conf. Proc. C **7902131** (1979) 95–99.
- [3] M. Gell-Mann, P. Ramond, and R. Slansky, *Complex Spinors and Unified Theories*, Conf. Proc. C **790927** (1979) 315–321, [arXiv:1306.4669 \[hep-th\]](#).
- [4] M. Fukugita and T. Yanagida, *Baryogenesis Without Grand Unification*, *Phys. Lett. B* **174** (1986) 45–47.
- [5] **Planck** Collaboration, N. Aghanim *et al.*, *Planck 2018 results. VI. Cosmological parameters*, *Astron. Astrophys.* **641** (2020) A6, [arXiv:1807.06209 \[astro-ph.CO\]](#). [Erratum: *Astron. Astrophys.* 652, C4 (2021)].

- [6] V. A. Kuzmin, V. A. Rubakov, and M. E. Shaposhnikov, *On the Anomalous Electroweak Baryon Number Nonconservation in the Early Universe*, *Phys. Lett. B* **155** (1985) 36.
- [7] F. R. Klinkhamer and N. S. Manton, *A Saddle Point Solution in the Weinberg-Salam Theory*, *Phys. Rev. D* **30** (1984) 2212.
- [8] R. Adhikari and U. Sarkar, *Baryogenesis in a supersymmetric model without R-parity*, *Phys. Lett. B* **427** (1998) 59–64, [arXiv:hep-ph/9610221](#).
- [9] T. Hambye, *Leptogenesis at the TeV scale*, *Nucl. Phys. B* **633** (2002) 171–192, [arXiv:hep-ph/0111089](#).
- [10] A. Dasgupta, P. S. Bhupal Dev, S. K. Kang, and Y. Zhang, *New mechanism for matter-antimatter asymmetry and connection with dark matter*, *Phys. Rev. D* **102** (2020) 055009, [arXiv:1911.03013](#) [[hep-ph](#)].
- [11] W. Abdallah, A. Kumar, and A. K. Saha, *Soft leptogenesis in the NMSSM with a singlet right-handed neutrino superfield*, *JHEP* **04** (2020) 065, [arXiv:1911.03363](#) [[hep-ph](#)].
- [12] D. Borah, A. Dasgupta, and D. Mahanta, *Dark Sector Assisted Low Scale Leptogenesis from Three Body Decay without Loops*, [arXiv:2008.10627](#) [[hep-ph](#)].
- [13] M. Le Dall and A. Ritz, *Leptogenesis and the Higgs Portal*, *Phys. Rev. D* **90** (2014) 096002, [arXiv:1408.2498](#) [[hep-ph](#)].
- [14] J. A. Casas and A. Ibarra, *Oscillating neutrinos and  $\mu \rightarrow e, \gamma$* , *Nucl. Phys. B* **618** (2001) 171–204, [arXiv:hep-ph/0103065](#).
- [15] **Particle Data Group** Collaboration, P. A. Zyla *et al.*, *Review of Particle Physics*, *PTEP* **2020** (2020) 083C01.
- [16] S. Davidson, E. Nardi, and Y. Nir, *Leptogenesis*, *Phys. Rept.* **466** (2008) 105–177, [arXiv:0802.2962](#) [[hep-ph](#)].
- [17] R. Kumar, *Covariant phase-space calculations of n-body decay and production processes*, *Phys. Rev.* **185** (1969) 1865–1875.
- [18] A. Granelli, K. Moffat, and S. T. Petcov, *Aspects of High Scale Leptogenesis with Low-Energy Leptonic CP Violation*, [arXiv:2107.02079](#) [[hep-ph](#)].
- [19] L. J. Hall, K. Jedamzik, J. March-Russell, and S. M. West, *Freeze-In Production of FIMP Dark Matter*, *JHEP* **03** (2010) 080, [arXiv:0911.1120](#) [[hep-ph](#)].
- [20] Y. Chikashige, R. N. Mohapatra, and R. Peccei, *Spontaneously Broken Lepton Number and Cosmological Constraints on the Neutrino Mass Spectrum*, *Phys. Rev. Lett.* **45** (1980) 1926.
- [21] Y. Chikashige, R. N. Mohapatra, and R. Peccei, *Are There Real Goldstone Bosons Associated with Broken Lepton Number?*, *Phys. Lett. B* **98** (1981) 265–268.
- [22] G. Gelmini and M. Roncadelli, *Left-Handed Neutrino Mass Scale and Spontaneously Broken Lepton Number*, *Phys. Lett. B* **99** (1981) 411–415.

- [23] C. D. Froggatt and H. B. Nielsen, *Hierarchy of Quark Masses, Cabibbo Angles and CP Violation*, *Nucl. Phys. B* **147** (1979) 277–298.
- [24] F. Wilczek, *Axions and Family Symmetry Breaking*, *Phys. Rev. Lett.* **49** (1982) 1549–1552.
- [25] L. Bento and J. W. F. Valle, *The Simplest model for the 17-KeV neutrino and the MSW effect*, *Phys. Lett. B* **264** (1991) 373–380.
- [26] E. Ma and R. Srivastava, *Dirac or inverse seesaw neutrino masses with  $B - L$  gauge symmetry and  $S_3$  flavor symmetry*, *Phys. Lett. B* **741** (2015) 217–222, [arXiv:1411.5042 \[hep-ph\]](#).
- [27] Y. Abe, Y. Hamada, T. Ohata, K. Suzuki, and K. Yoshioka, *TeV-scale Majorogenesis*, *JHEP* **07** (2020) 105, [arXiv:2004.00599 \[hep-ph\]](#).
- [28] S. Matsumoto and K. Yoshioka, *Deep Correlation Between Cosmic-Ray Anomaly and Neutrino Masses*, *Phys. Rev. D* **82** (2010) 053009, [arXiv:1006.1688 \[hep-ph\]](#).
- [29] R. Barbieri, P. Creminelli, A. Strumia, and N. Tetradis, *Baryogenesis through leptogenesis*, *Nucl. Phys. B* **575** (2000) 61–77, [arXiv:hep-ph/9911315](#).
- [30] W. Buchmuller, P. Di Bari, and M. Plumacher, *Some aspects of thermal leptogenesis*, *New J. Phys.* **6** (2004) 105, [arXiv:hep-ph/0406014](#).